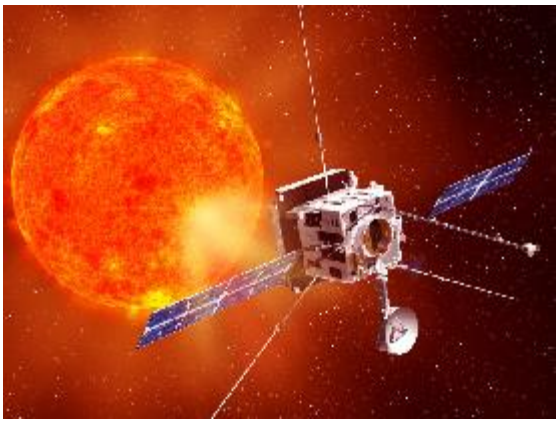

SOLAR ORBITER ENERGETIC PARTICLE DETECTOR

EPT-HET Structural Analysis Report

Document ID: SO-EPD-KIE-RP-0040

Issue: 3

Revision: 3

Date: 2014-04-23

Signature not needed if electronically approved by route					
Written	**Checked**	**Approved Configuration Control**	**Approved QA**	**Approved Experiment Manager**	**Approved Principal Investigator**
Félix Sorribes 2014-04-23	**Gustavo Alonso 2014-04-23**	**NAME3 Date and Signature**	**NAME4 Date and Signature**	**NAME5 Date and Signature**	**NAME6 Date and Signature**

File: SO-EPD-KIE-RP-0040-iss3_rev3-EPT-HET-Structural_Analysis_Report **Pages:** 65

DISTRIBUTION LIST

The following lists indicate the individuals and agencies in receipt of review copies of the present document:

Agency / Organization	Name & Title	Contact information
SRG-UAH	Javier Rodríguez-Pacheco EPD- Principal Investigator	javier.pacheco@uah.es
SRG-UAH	Manuel Prieto EPD Project Manager	manuel.prieto@uah.es
SRG-UAH	Cecilia Gordillo EPD Configuration Control Responsible	cecilia.gordillo@uah.es
SRG-UAH	Andrés Russu Berlanga EPD System Engineer	Andres.Russu@uah.es
SENER	Giuseppe Penestri EPD System Engineer	giuseppe.pennestri@sener.es
SENER	Mario Basile EPD Product Assurance Manager	mario.basile@sener.es
IDR/UPM	Gustavo Alonso Isabel Pérez Structural and Thermal Mathematical Models	gustavo.alonso@upm.es isabel.perez.grande@upm.es
CAU	Michael Richards EPD/Kiel Product Assurance Manager	mir@richards-consulting.eu
CAU	EPD Kiel Team	solo_kiel@physik.uni-kiel.de

CHANGES RECORD

Issue	Revision	Date	Modified by	Section / Paragraph modified	Change implemented
1	0	13/10/2011		All	Initial release
1	1	16/12/2011	C. Martin		Formal changes, removing yellow review markers
2	0	26/05/2013	G. Fernandez	Major changes / Most sections	PDR RIDs updating
3	0	27/09/2013	F. Sorribes	Major changes / Most sections	CDR
3	1	30/10/2013	F. Sorribes	Minor changes/ Most sections	Following observations from KU (R-KIE)
3	2	26/11/2013	F. Sorribes	Sec. 6	After STEP pre-CDR Applying EIDA-i4 random vibration levels
3	3	30/04/2014	A. García	List of figures/ List of tables	New
				Sec. 4 and Sec. 5	Indication of CS1 Coordinate System (CDR 222)
					Table 4-1: Introduction of T^aref and CTE (CDR-222)
					Updating results (mass, properties, CoM, checks) with the latest FEM version
				Sec. 6.2	New section: Quasi-Static analysis
				Sec. 6.3	Introduction of stress results table and stress distribution figures for sine vibration
				Sec. 6.4	Introduction of stress results table and stress distribution figures for random vibration
				Sec. 6.5	QS Bolt analysis
				Sec 6.6	New section: Standoff crush analysis (CDR-224)
				Sec. 7	New section: Fail-Safe analysis (CDR-225)

TABLE OF CONTENTS

1 APPLICABLE AND REFERENCE DOCUMENTS 9
1.1 Applicable Documents 9
1.2 Reference Documents 9
2 SCOPE 10
3 GLOSARY AND DEFINITIONS 11
3.1 Acronyms and Abbreviations 11
4 DESCRIPTION 12
4.1 Overall Description 12
4.2 Unit System 12
4.3 Coordinate Systems 12
4.4 Mass and CoM Budget 13
4.5 Material Characteristics 13
5 FE MODEL 15
5.1 FEM Code and Pre/Post Processors 15
5.2 FEM Units 15
5.3 FEM Coordinate Systems 15
5.4 FE Model Description 15
5.4.1 Assumptions and idealizations 15
5.4.2 Geometry 15
5.4.3 Interfaces 17
5.4.4 Boundary Conditions 17
5.4.5 Properties and Materials 18
5.4.6 Mass Distribution Summary 20
5.4.7 Non linearity 21
5.4.8 Other special modeling features 21
5.5 FEM/Model Checks 22
5.5.1 Pre-run checks 22
5.5.2 Gravity load check 22
5.5.3 Rigid body frequency check 22
5.5.4 Strain energy check 23
6 ANALYSES 26
6.1 Normal Modes Analysis 26
6.2 Quasi-static analysis 32
6.3 Sine Vibration Analysis 40
6.4 Random Vibration Analysis 46
6.5 Bolt Analysis 51
6.5.1 Margin of safety on tensile failure 51
6.5.2 No gapping criteria 52
6.5.3 No sliding criteria 53
6.5.4 Margin of safety on fastener shear failure 53
6.6 Standoff crush analysis 54

7 FAIL-SAFE ANALYSIS 56

7.1 Normal mode analysis 56
7.2 Cuasi-static analysis 60
7.3 Bolt failure 61
7.3.1 Margin of safety on tensile failure 61
7.3.2 No gapping criteria 62
7.3.3 No sliding criteria 62
7.3.4 Margin of safety on fastener shear failure 63

8 CONCLUSIONS 65

List of figures

Figure 4-1 CAD model (left) and PATRAN Geometry (right).....12
Figure 4-2 Coordinate System.....13
Figure 5-1 Power Module v1 and baseplate CAD model (left) and PATRAN Geometry (right).....16
Figure 5-2 Power Module v2 and EPT baseplate CAD model (left) and PATRAN Geometry (right).....16
Figure 5-3 HET housing CAD model (left) and PATRAN Geometry (right).....16
Figure 5-4 Interface nodes. 17
Figure 5-5 Shell thickness distribution.....19
Figure 5-6 Non-structural mass distribution.....20
Figure 5-7 Principal axes of inertia of the FEM model at CoM.....21
Figure 6-1 First Mode (348 Hz). 26
Figure 6-2 Second mode (350 Hz). 27
Figure 6-3 Third Mode (360 Hz). 27
Figure 6-4 Fourth Mode (419 Hz). 28
Figure 6-5 Fifth Mode (476 Hz). 28
Figure 6-6 Sixth Mode (533 Hz). 28
Figure 6-7 Modal effective masses fractional and accumulated – Translational DoFs.....30
Figure 6-8 Modal effective masses fractional and accumulated – Rotational DoFs. 31
Figure 6-9 Quasi-Static specification.....32
Figure 6-10 Maximum Von Mises stress for Al 6061-T6 structure - Quasi-Static in X.....33
Figure 6-11 Maximum Von Mises stress for Al 6061-T6 structure - Quasi-Static in Y.....33
Figure 6-12 Maximum Von Mises stress for Al 6061-T6 structure - Quasi-Static in Z. 34
Figure 6-13 Maximum Von Mises stress for PCB - Quasi-Static in X. 34
Figure 6-14 Maximum Von Mises stress for PCB - Quasi-Static in Y. 35
Figure 6-15 Maximum Von Mises stress for PCB - Quasi-Static in Z. 35
Figure 6-16 Sine Vibration test levels – EPT/HET. 40
Figure 6-17 Maximum Von Mises stress for Al 6061-T6 structure – Sine Vibration in X. 42
Figure 6-18 Maximum Von Mises stress for Al 6061-T6 structure – Sine Vibration in Y. 42
Figure 6-19 Maximum Von Mises stress for Al 6061-T6 structure – Sine Vibration in Z. 43
Figure 6-20 Maximum Von Mises stress for PCB – Sine Vibration in X.....43
Figure 6-21 Maximum Von Mises stress for PCB – Sine Vibration in Y.....44
Figure 6-22 Maximum Von Mises stress for PCB – Sine Vibration in Z.....44
Figure 6-23 Random Vibration test levels – EPT/HET.....46
Figure 6-24 Maximum Von Mises (3 x RMS) stress for Al 6061-T6 structure – Random Vibration in X. 48
Figure 6-25 Maximum Von Mises (3 x RMS) stress for Al 6061-T6 structure – Random Vibration in Y. 48
Figure 6-26 Maximum Von Mises (3 x RMS) stress for Al 6061-T6 structure – Random Vibration in Z.....49
Figure 6-27 Maximum Von Mises (3 x RMS) stress for PCB – Random Vibration in X.....49

Figure 6-28 Maximum Von Mises (3 x RMS) stress for PCB – Random Vibration in Y. 50
Figure 6-29 Maximum Von Mises (3 x RMS) stress for PCB – Random Vibration in Z. 50
Figure 7-1 Modal effective masses fractional and accumulated – Translational DoF. 57
Figure 7-2 Modal effective masses fractional and accumulated – Rotational DoF. 58
Figure 7-3 First mode (276.3 Hz). 59
Figure 7-4 Fifth mode (395.21 Hz). 59
Figure 7-5 Sixth mode (513.3Hz). 60

List of tables

Table 1-1 Applicable Documents. 9
Table 1-2 Reference Documents. 9
Table 4-1 Material Properties. 14
Table 5-1 Interfaces nodes numbering range and location. 17
Table 5-2 Interfaces SPC corresponding nodes. 18
Table 5-3 CQUAD4 and CTRIA3 Shell type element properties and range. 18
Table 5-4 CBAR type element properties and range. 19
Table 5-5 lumped element mass (CONM2) properties and numbering range 19
Table 5-6 mass distribution summary. 20
Table 5-7 Center of mass in CS1 (FEM). 20
Table 5-8 Center of mass in URF≡ CS1 (MICD) 21
Table 5-9 Moments of inertia in CS1. 21
Table 5-10 Rigid body modes frequencies. 23
Table 5-11 Results of rigid body checks of matrix KGG. 23
Table 5-12 Results of rigid body checks of matrix KNN. 24
Table 5-13 Results of rigid body checks of matrix KFF. 24
Table 5-14 Results of rigid body checks of matrix KAA1. 25
Table 5-15 Results of support strain energy. 25
Table 6-1 Natural frequencies of the constrained FEM. 26
Table 6-2 Eigenfrequencies and associated modal effective masses – Traslational DoFs. 29
Table 6-3 Eigenfrequencies and associated modal effective masses – Rotational DoFs. 31
Table 6-4 Mass-Acceleration (g). 32
Table 6-5 Von Mises Maximum Stresses and BAR Maximum combined Stresses for Quasi-Static analysis. 32
Table 6-6 Safety factors. 36
Table 6-7 Margins of Safety for Quasi-Static Analysis. 36
Table 6-8 Quasi-Static Analysis X, Y, Z – I/F forces. 37
Table 6-9 Mass acceleration (g). 37

Table 6-10 Von Mises Maximum Stresses and BAR Maximum combined Stresses. 38
Table 6-11 Margins of Safety for Combined Quasi-Static Analysis. 38
Table 6-12 Combined Quasi-Static resultant loads – I/F Forces. 39
Table 6-13 Sine Vibration test levels – EPT/HET. 40
Table 6-14 Sine Vibration analysis – I/F Forces. 41
Table 6-15 Sine Vibration analysis – Maximum stresses. 41
Table 6-16 Margins of Safety for Sine Vibration Analysis. 45
Table 6-17 Random Vibration test levels – EPT/HET. 46
Table 6-18 Random Vibration analysis – I/F RMS Forces. 47
Table 6-19 Random Vibration analysis – Maximum stresses in the structure. 47
Table 6-20 Margins of Safety for Random Vibration Analysis. 51
Table 6-21 Worst conditions of the combined Quasi-Static cases - I/F loads. 51
Table 6-22 Margins of Safety on bolt tensile failure. 52
Table 6-23 Margins of Safety on gapping. 53
Table 6-24 Margins of Safety on sliding. 53
Table 6-25 Margin of safety on fastener shear failure. 54
Table 6-26 Margin of Safety on Standoff crushing – Minimum value 55
Table 7-1 Eigenfrequencies and associated modal effective masses – Traslational DoFs. 57
Table 7-2 Eigenfrequencies and associated modal effective masses – Rotational DoFs. 58
Table 7-3 Mass acceleration (g). 60
Table 7-4 Combined Quasi-Static resultant loads X, Y, Z – I/F Forces. 61
Table 7-5 Margins of Safety on bolt tensile failure – Minimum value. 62
Table 7-6 Margins of Safety on gapping – Minimum value. 62
Table 7-7 Margins of Safety on sliding – Minimum values. 63
Table 7-8 Margins of Safety on fastener shear failure. 64

1 APPLICABLE AND REFERENCE DOCUMENTS

1.1 Applicable Documents

ID.	Title	Reference	Iss./Rev.	Date
AD1	Experiment Interface Document part A	SOL.EST.RCD.0050_04	4/0	13/06/2013
AD2	Experiment Interface Document part B	SO-EPD-PO-IF-00001	3/2 DRAFT	05/03/2013
AD3	ECSS-E-30_Part-2A-Mechanical_Part-2-Structural	-	-	25/04/2000
AD4	SOLAR ORBITER: Mechanical FEM Requirement Specification	SOL.S.ASTR.RS.00011	2/0	30/09/2011
AD5	Generic Mechanical FEM Specification	ADS.E.0787	2/0	24/01/2008
AD6	Data for selection of space materials and processes	ECSS-Q-70-71A	rev 1	18/06/2004

Table 1-1 Applicable Documents.

1.2 Reference Documents

ID.	Title	Reference	Iss./Rev.	Date
RD1	so-EPT-HET-c3_top.stp			20/07/2011
RD2	so_epthet_mass-estimation_v4_excerpt_upm-cdr-update			09/10/2013
RD3	EPT-HET Mechanical Interface Control Drawing	SO-EPD-KIE-DR-0001	3/0	17/02/2011
RD4	SO-EPD-KIE-TR-0005_iss1_rev0_EPT-HET_STM_Vibration-test-procedure.pdf	SO-EPD-KIE-TR-0005	1/0	2/09/2013
RD5	20131016_CAU_IDRUPM_review_EPT-HET_structural_analysis_issue_3_CDR.pdf	R-KIE	1	16/10/2013
RD6	Experiment Interface Document part A	SOL.EST.RCD.0050_02	2/8	14/10/2011

Table 1-2 Reference Documents.

2 SCOPE

This document is intended to respond the EPD EPT-HET CDR actions regarding the structural analysis.

3 GLOSARY AND DEFINITIONS

3.1 Acronyms and Abbreviations

CAD	Computer Aided Design
CoM	Center of Mass
CONM2	CONcentrated Mass element, form 2
CQUAD4	QUADrilateral plate element with 4 grids
DoF	Degree of Freedom
EPD	Energetic Particles Detector
EPT	Electron, Proton Telescope
EPT-HET	Electron Proton Telescope – High Energy Telescope
FE	Finite Element
FEM	Finite Element Model
FOSY	Yield Factor Of Safety
FOSU	Ultimate Factor Of Safety
HET	High Energy Telescope
ID.	Identification
I/F	Interface
MEM	Modal effective mass
MICD	Mechanical Interface Control Drawing
MOS	Margin Of Safety
MPC	Multi Point Constraint
PDR	Preliminary Design Review
RBE2	Rigid Body Element, form 2
RID	Review Item Discrepancy
SMM	Structural Mathematical Model
SO	Solar Orbiter
SPC	Single Point Constraint
URF	Unit Reference Frame

4 DESCRIPTION

The SMM construction is explained in this chapter. A general description is offered, including geometry, coordinate and unit systems, mass budget and material characteristics.

4.1 Overall Description

The models geometry has been built following the .stp file provided by the EPT-HET team [RD1] and the mass estimation [RD2]. Although global dimensions have been used, the complex geometrical shapes have been substituted by flat surfaces, and instruments which do not contribute to the structural strength or stiffness by lumped mass elements (CONM2), resulting in a simple Patran® geometry.

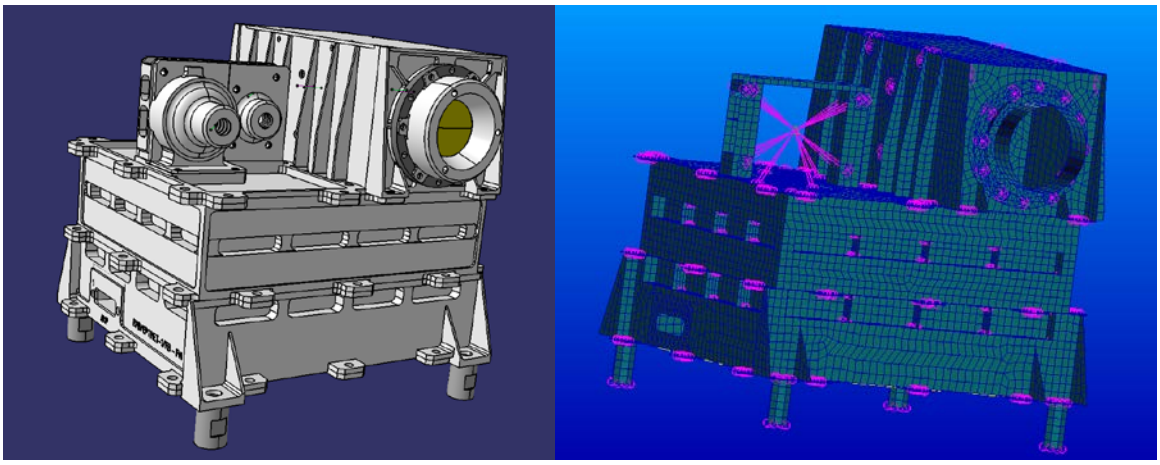

Figure 4-1 CAD model (left) and PATRAN Geometry (right).

4.2 Unit System

The FEM model has been established with International System of measurement units (meter, kilogram, second, Newton, radian, Celsius degree), as required in [AD5].

4.3 Coordinate Systems

According with [AD4], the EPD SMM, in particular EPT-HET SMM, does not have to be implemented in a higher hierarchy SMM.

The coordinate system defined in the EPT-HET SMM (CS1) is the same as the coordinate system used in the CAD Model (EPT-HET MICD [RD3]). The axes of the coordinate system are shown in Figure 4-2.Thus, all the FEM grids have been referenced to the CS1.

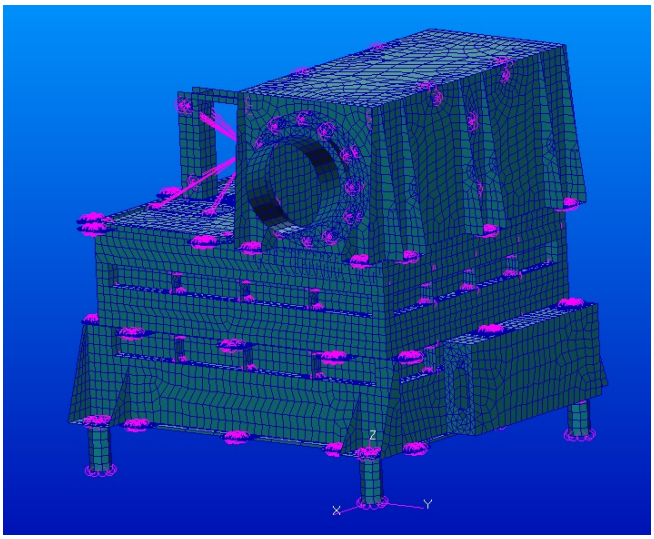

Figure 4-2 Coordinate System.

4.4 Mass and CoM Budget

For the non-structural elements, the masses reported in the mass estimation [RD2] have been used. For the structural elements, as they have been shell-like modeled, mean thicknesses have been obtained from the provided CAD model [RD1].

4.5 Material Characteristics

These are the materials that have been used in the model. The temperature reference for all the materials is 20ºC.

Material Name	Property	Value	Units
Ti_6Al_4V	Density	4430	kg/m^3
	Modulus of Elasticity	113.8E+09	Pa
	Poisson's ratio	0.342	N/A
	Yield tensile strength	847	MPa
	Ultimate tensile strength	924	MPa
	Thermal expansion coefficient	8.6	µm/mK
Al_6061-T6	Density	2710	kg/m^3
	Modulus of Elasticity	68.9E+09	Pa

Al_6061-T6	Poisson's ratio	0.330	N/A
	Yield tensile strength	276	MPa
	Ultimate tensile strength	310	MPa
	Thermal expansion coefficient	23.5	µm/mK
Ultem	Density	1270	kg/m^3
	Modulus of Elasticity	3.2E+09	Pa
	Poisson's ratio	0.3	N/A
	Yield tensile strength	155	MPa
	Ultimate tensile strength	165	MPa
	Thermal expansion coefficient	30	µm/mK
PCB (FR4)	Density	1850	kg/m^3
	Modulus of Elasticity	20.1E+09	Pa
	Poisson's ratio	0.118	N/A
	Yield tensile strength	310	MPa
	Ultimate tensile strength	345	MPa
	Thermal expansion coefficient	20	µm/mK

Table 4-1 Material Properties.

5 FE MODEL

5.1 FEM Code and Pre/Post Processors

The code employed for the analysis has been MSC NASTRAN 2013.1. Pre/post processors adopted have been MSC PATRAN 2012.2.2.

5.2 FEM Units

The FEM model has been established with International System of measurement units (meter, kilogram, second, Newton, radian, Celsius degree), as required in [AD5].

5.3 FEM Coordinate Systems

As was explained in section 4.3, the coordinate system used in the EPT-HET SMM is the same that which was defined in EPT-HET MICD [RD3]. Thus, all the FEM grids have been referenced to the CS1.

5.4 FE Model Description

5.4.1 Assumptions and idealizations

The complex geometrical shapes that can be found in the early CAD model [RD1] have been idealized as 2D shell-like (CQUAD4 & CTRIA3). Also, to join adjacent parts of the structure, RBE2 MPCs have been used following the guidelines given by [AD5]. That is with respect to the elements which play a structural role in the instrument. Elements which do not contribute to structural stiffness have been modeled either as lumped elements (CONM2) joined to the structure by RBE2 type MPCs.

The thicknesses of the different shells have been chosen to make the model mass compliant with the CAD model provided.

All the mathematical models are linear, as it is said in [AD4] and [AD5].

5.4.2 Geometry

Global dimensions have been used. The FEM models geometry is compliant with [RD1] and [RD3].

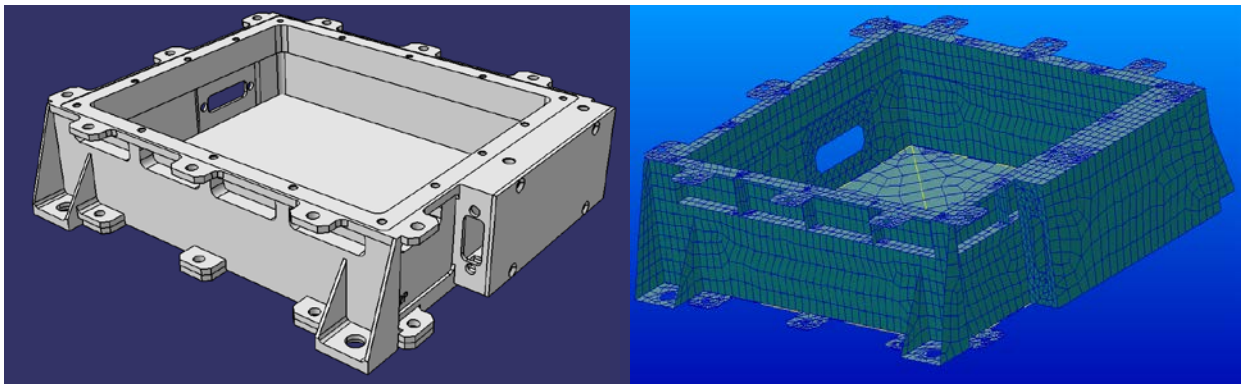

Figure 5-1 Power Module v1 and baseplate CAD model (left) and PATRAN Geometry (right).

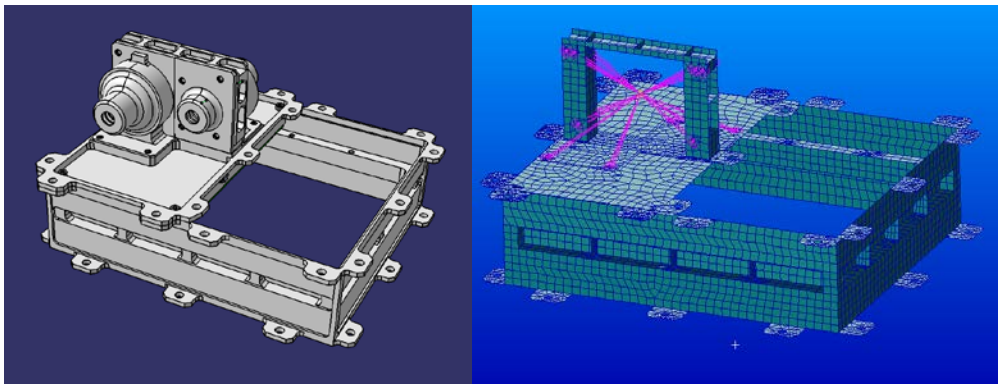

Figure 5-2 Power Module v2 and EPT baseplate CAD model (left) and PATRAN Geometry (right).

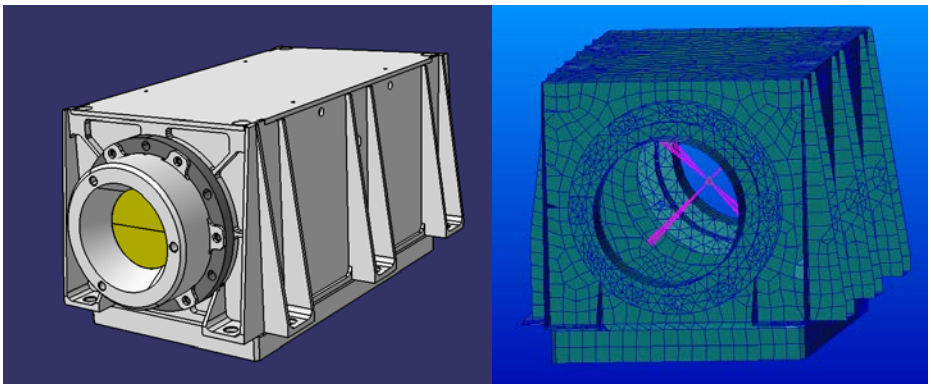

Figure 5-3 HET housing CAD model (left) and PATRAN Geometry (right).

Unions between not coincident nodes have been modeled using MPCs of RBE2 type, as stated in [AD5]. The total number of them is 179. The lumped masses have been spread over the structure via CONM2 cards (8) with no offset, and joined to it via RBE2 cards.

5.4.3 Interfaces

The interfaces to the SO deck have been designed according to specifications included in [AD5]. These are 4xM5 screws of Ti6Al4V inside the mounting area. Their coordinates in the CS1 (instrument MICD) coordinate system are:

Node	X_{CS1} (mm)	Y_{CS1} (mm)	Z_{CS1} (mm)
100000	0.0	-114.95	0.0
100007	0.0	0.0	0.0
100014	-116.0	0.05	0.0
100021	-115.97	114.92	0.0

Table 5-1 Interfaces nodes numbering range and location.

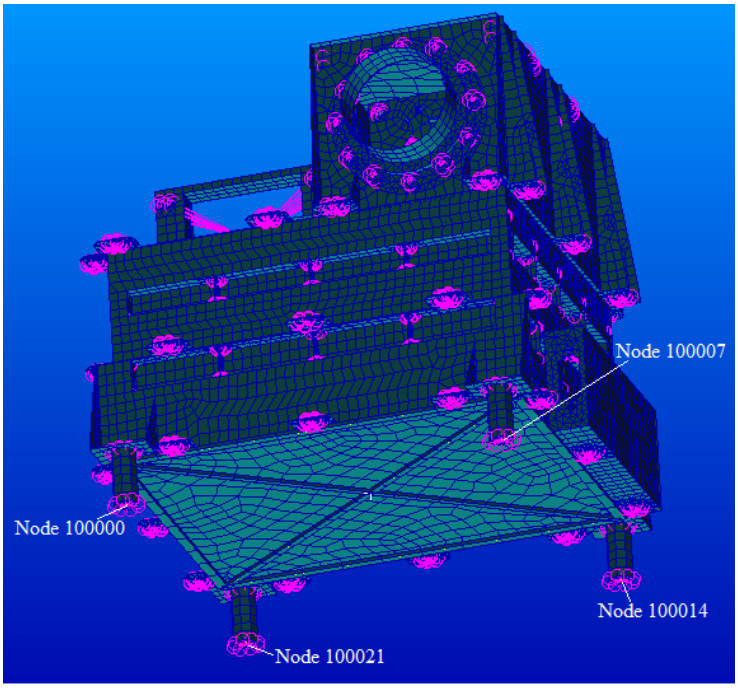

Figure 5-4 Interface nodes.

5.4.4 Boundary Conditions

The boundary conditions on the interfaces with SO deck should represent the attachment with bolts of the EPT-HET to the SO deck. This is, constraining the three translational and the two out-of-plane rotational degrees of freedom on the interface nodes.

I/F	Nodes
1	100000
2	100007
3	100014
4	100021

Table 5-2 Interfaces SPC corresponding nodes.

The interface bolts are made of Ti-6Al-4V, its total mass is 0.006 kg and the element range is 100000 – 100023. The Ultem standoffs total mass is 0.004 kg and the element range is 100206 – 100397.

5.4.5 Properties and Materials

Materials are the aforementioned in Table 4-1. Al 6061-T6 has been used for the 2D shell properties for the main EPT-HET structure. PCB has been used for the 2D shell properties for the 5 electronic boards. Under these lines a description of the properties, their characteristics and their numbering range can be found in Table 5-3. The elements used in the model are CQUAD4 (14486), CTRIA3 (10010), CBAR(218) and CONM2 (2).

Prop. Set Name	Thickness (mm)	Mass (kg)	CAD Assoc. Element	Num. Range
Ebox_bottom_plate	1	0.046	so-epthet-c5-2227-ls_bottom-plate	101000 – 102836
Ebox_power_mod	1, 2, 2.5, 4, 5	0.311	so-ept-het-c5_2311_ebox-power-module	108000 – 112637
Ebox_data_mod	1, 2, 4.1	0.075	so-ept-het-c5_2215_ebox-power-module	130000 – 134173
EPT_baseplate	1, 2, 5, 6	0.047	so-ept-c8-2219_base-plate	140000 – 143112
HET_bgocap	2, 5	0.043	so-het-c12-2232_bgocap so-het-c12-2233_bgocap	145000 – 146005
HET_housing	1, 1.5, 2, 7	0.169	so-het-c12-2220_housing_1	150000 – 156111
Board 1	1.6	0.143	so-epthet-c5_2252_power-board	105000 – 105844
Board 2	1.6	0.143	so-epthet-c5_2251_digital-board	115000 – 115840
Board 3	1.6	0.143	so-epthet-c5_2250_analog-adc-shaper-board	118000 – 118840
Board 4	1.6	0.049	so-ept-c8_226_preamp-boad	120000 – 121083
Board 5	1.6	0.132	so-het-c12_2228_preamp-pcb	122000 – 123083
BoardCarrier	2.5	0.018	so-ept-c8_2214_board-carrier-1	125000 – 126020
Ultem_Ebox_feet	2.25	0.004	so_het_c5_2221_therm_standoff	100206 – 100397

Table 5-3 CQUAD4 and CTRIA3 Shell type element properties and range.

Prop. Set Name	Mass (kg)	CAD Assoc. Element	Num. Range
Epthet_screw_Ti_6Al_4V_M5	0.006	so_het_c5_2221_therm_standoff	100000:100023

Table 5-4 CBAR type element properties and range.

Two CONM2 elements have been used for modeling two components of the EPT-HET. These CONM2 elements have the same mass properties (mass, moments of inertia) as the hardware they represent.

Prop. Set Name	Mass (kg)	CAD Assoc. Element	Num. Range
EPT_telescope	0.113	so-ept-c8_telescope_v1	200000
HET_telescope	0.150	so-het-c9-00_top_1	200001

Table 5-5 lumped element mass (CONM2) properties and numbering range

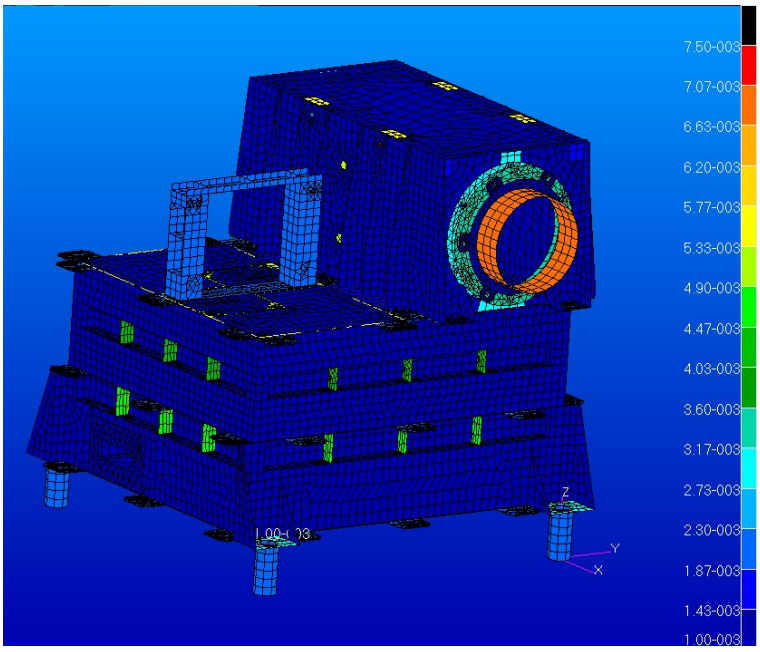

Figure 5-5 Shell thickness distribution.

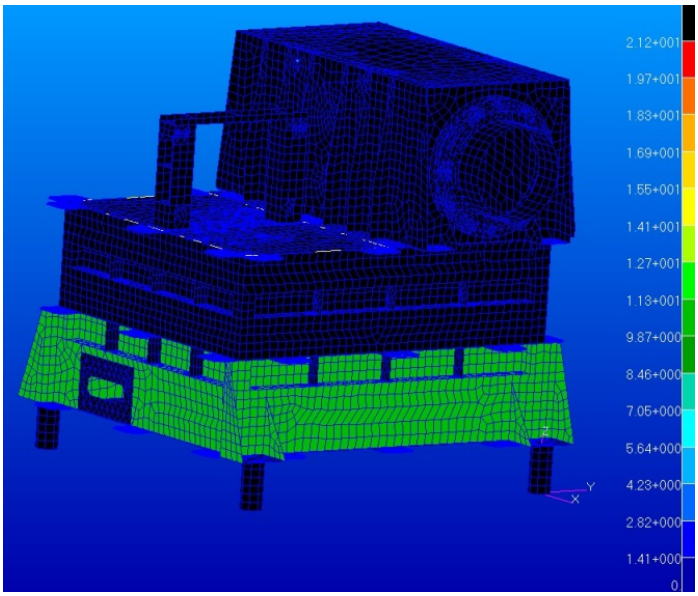

Figure 5-6 Non-structural mass distribution.

5.4.6 Mass Distribution Summary

As the mass distribution was shown as the element properties, in this section we will just add them all to make the total. So, the mass distribution divided in different type properties is:

Property type	Mass [kg]
CQUAD4 + TRIA3	1.329
CONM2	0.263
Total	1.592

Table 5-6 mass distribution summary.

The total mass of the FEM matches with the mass specified in the mass budget [RD2]. The masses of the placeholers and screws are distributed as a non structural mass mainly in the power modele and in the PCB boards.The CoM of the FEM CS1 is:

X_{CS1} (mm)	Y_{CS1} (mm)	Z_{CS1} (mm)
-58.2	-49.9	67.3

Table 5-7 Center of mass in CS1 (FEM).

The CoM of the EPT-HET instrument URF in the MICD [RD3] is:

X_{URF} (mm)	Y_{URF} (mm)	Z_{URF} (mm)
-55.2	-54.8	65.0

Table 5-8 Center of mass in URF≡ CS1 (MICD)

And the principal moments of inertia at center of mass is:

Ix_{CS1} (kg·m^2)	Iy_{CS1} (kg·m^2)	Iz_{CS1} (kg·m^2)
4.44E-3	3.36E-3	4.29E-3

Table 5-9 Moments of inertia in CS1.

The coordinate system CS1 in FE Model coincide with the coordinate system of the CAD model. The maximum deviation between the coordinates of the CoM in both models is approximately 3.5 %.

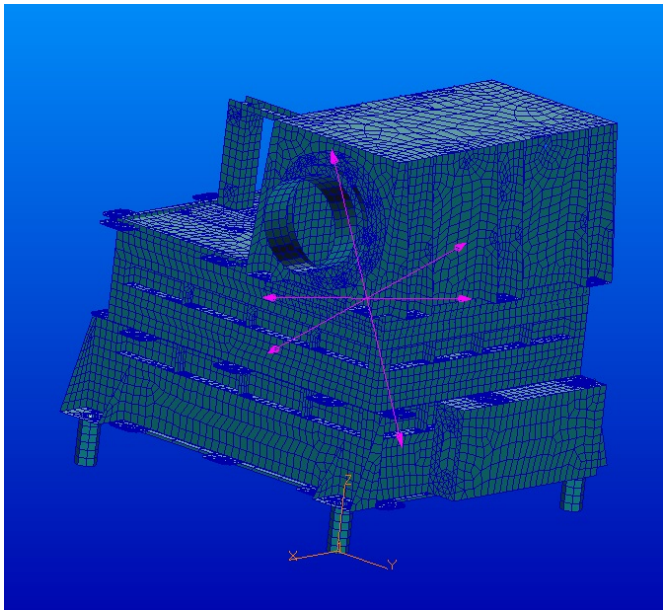

Figure 5-7 Principal axes of inertia of the FEM model at CoM.

5.4.7 Non linearity

All the mathematical models are linear.

5.4.8 Other special modeling features

N/A

5.5 FEM/Model Checks

5.5.1 Pre-run checks

For all the model checks, the pre-run checks have been performed:

1. Free nodes: there are no unconnected nodes.
2 Free Edges: there is no disconnection between model parts.
3. Element coincidence: there are no coincident elements.
4. Element shrink: there are no missing elements.
5. Element distortion: all element types are compliant with maximum distortion requirements.
6. Spring elements: none
7. Rigid elements: mathematical relations between DoF correct
8. Material properties: correctly simulated
9. Material orientation: no composites
10. Lumped masses: correctly located and no off-set
11. Pressure loads: none

5.5.2 Gravity load check

A 1 m/s^2 gravitation load was applied to FEM (constrained at its interface) separately in each of the X, Y, and Z CS1 axes directions.

X-Axis Direction:

- The SPCFORCE RESULTANT was -1.592 N in the applied direction, which is exactly the calculated mass (1.592 kg) multiplied by 1 m/s^2.
- The maximum displacements were of an order of 1E-6 meters.

Y-Axis Direction:

- The SPCFORCE RESULTANT was -1.592 N in the applied direction, which is exactly the calculated mass (1.592 kg) multiplied by 1 m/s^2.
- The maximum displacements were of an order of 1E-6 meters.

Z-Axis Direction:

- The SPCFORCE RESULTANT was -1.592 N in the applied direction, which is exactly the calculated mass (1.592 kg) multiplied by 1 m/s^2.
- The maximum displacements were of an order of 1E-6 meters.
-

5.5.3 Rigid body frequency check

The first six eigenvalues of the free-free normal modes analysis were under 0.005 Hz.

Mode	Frequency (Hz)
1º	8.26E-04
2º	6.62E-04
3º	2.56E-04
4º	2.59E-04
5º	5.71E-04
6º	8.54E-04

Table 5-10 Rigid body modes frequencies.

5.5.4 Strain energy check

A classical NASTRAN dynamic analysis (SOL 103) was performed with the model constrained using SUPORT card. The model was constrained by specification of sufficient degrees of freedom to eliminate rigid body motion. The results of the test performed with the NASTRAN GROUNDCHECK for the different sets are shown in Table 5-11 to Table 5-15:

G-set (limit = 1.0E-2 J):

Direction	Strain Energy (J)	Pass/Fail
1	1.87E-06	PASS
2	3.11E-06	PASS
3	6.06E-06	PASS
4	1.11E-08	PASS
5	1.93E-08	PASS
6	3.33E-10	PASS

Table 5-11 Results of rigid body checks of matrix KGG.

N-set (limit = 1.0E-2 J):

Direction	Strain Energy (J)	Pass/Fail
1	4.98E-06	PASS
2	4.64E-06	PASS
3	5.19E-06	PASS
4	8.83E-09	PASS
5	6.06E-08	PASS
6	1.49E-08	PASS

Table 5-12 Results of rigid body checks of matrix KNN.

F-set (limit = 1.0E-2 J for translational DoF and 5.0E-2J for rotational DoF):

Direction	Strain Energy (J)	Pass/Fail
1	4.98E-06	PASS
2	4.64E-06	PASS
3	5.18E-06	PASS
4	8.83E-09	PASS
5	6.06E-08	PASS
6	1.49E-08	PASS

Table 5-13 Results of rigid body checks of matrix KFF.

A-set (limit = 1.0E-2 J for translational DoF and 5.0E-2J for rotational DoF):

Direction	Strain Energy (J)	Pass/Fail
1	4.98E-06	PASS
2	4.64E-06	PASS
3	5.18E-06	PASS
4	8.83E-09	PASS

5	6.06E-08	PASS
6	1.49E-08	PASS

Table 5-14 Results of rigid body checks of matrix KAA1.

Support strain energy (limit = 5.0E-2 J):

Suport nº	Strain Energy (J)	Pass/Fail
1	1.45E-05	PASS
2	2.61E-06	PASS
3	-7.85E-06	PASS
4	-4.01E-08	PASS
5	-2.67E-08	PASS
6	3.77E-08	PASS

Table 5-15 Results of support strain energy.

6 ANALYSES

6.1 Normal Modes Analysis

A normal modes analysis of the constrained FEM was performed. The first modes are shown and some figures of them are depicted below. The first eigenfrequency has a value of 348.3 Hz, which is compliant with EID-A requirement (**EIDA R-089**) [AD1], which is that all fundamental resonance frequencies of the instrument should be above 140 Hz.

Mode	Frequency (Hz)	Mode	Frequency (Hz)	Mode	Frequency (Hz)
1º	348.3	8º	619.0	15º	774.2
2º	350.4	9º	619.4	16º	801.3
3º	360.6	10º	647.0	17º	812.5
4º	419.5	11º	660.8	18º	834.7
5º	476.4	12º	686.3	19º	866.8
6º	533.6	13º	725.7	20º	908.2
7º	542.3	14º	743.4	21º	1030.3

Table 6-1 Natural frequencies of the constrained FEM.

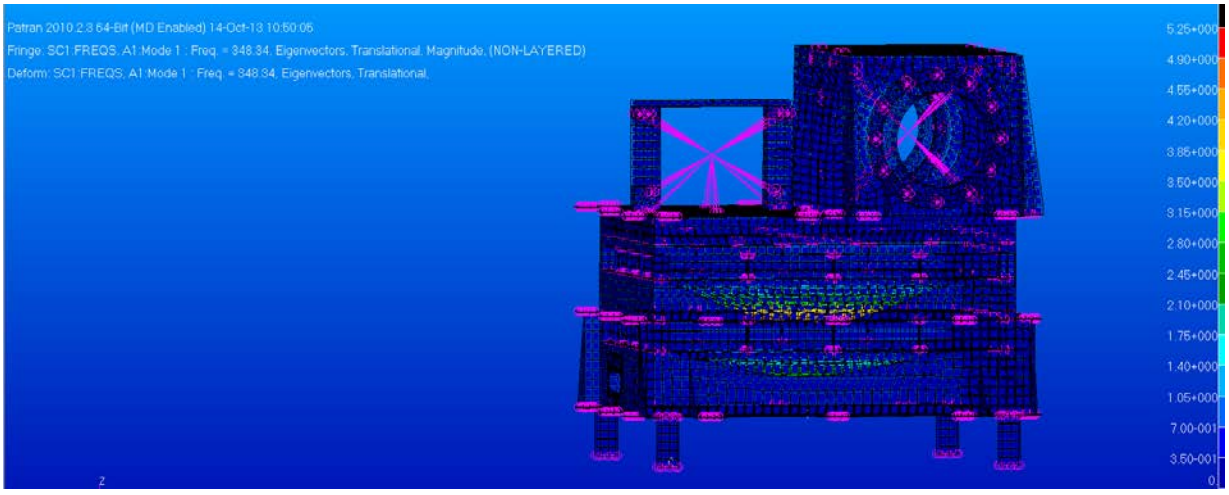

Figure 6-1 First Mode (348 Hz).

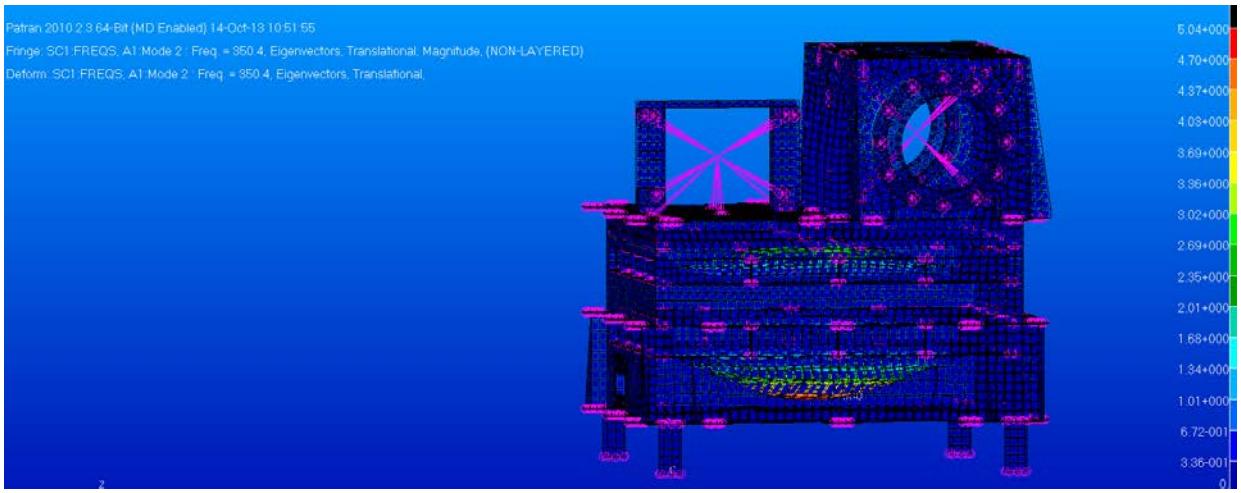

Figure 6-2 Second mode (350 Hz).

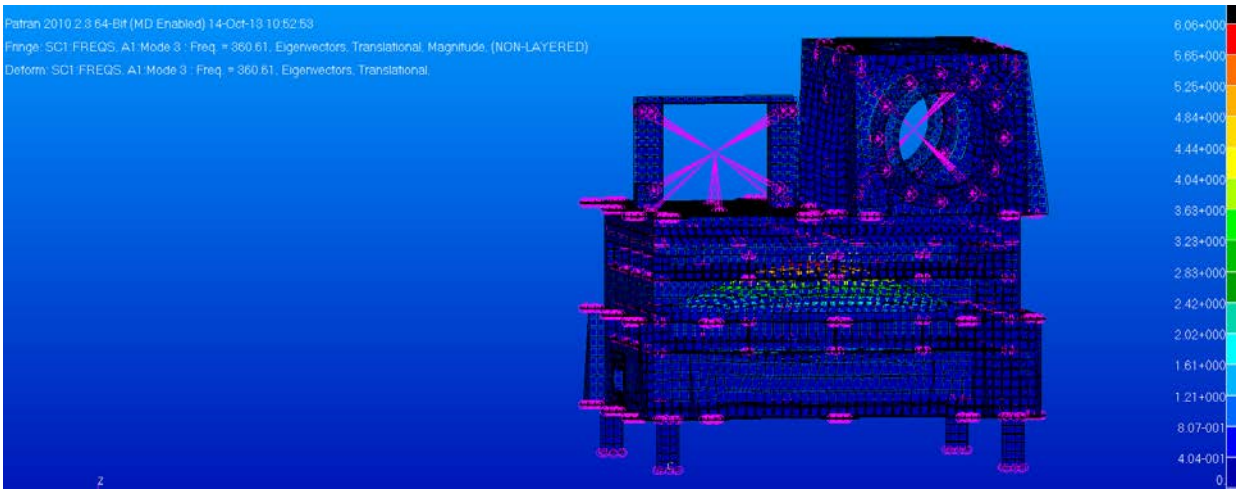

Figure 6-3 Third Mode (360 Hz).

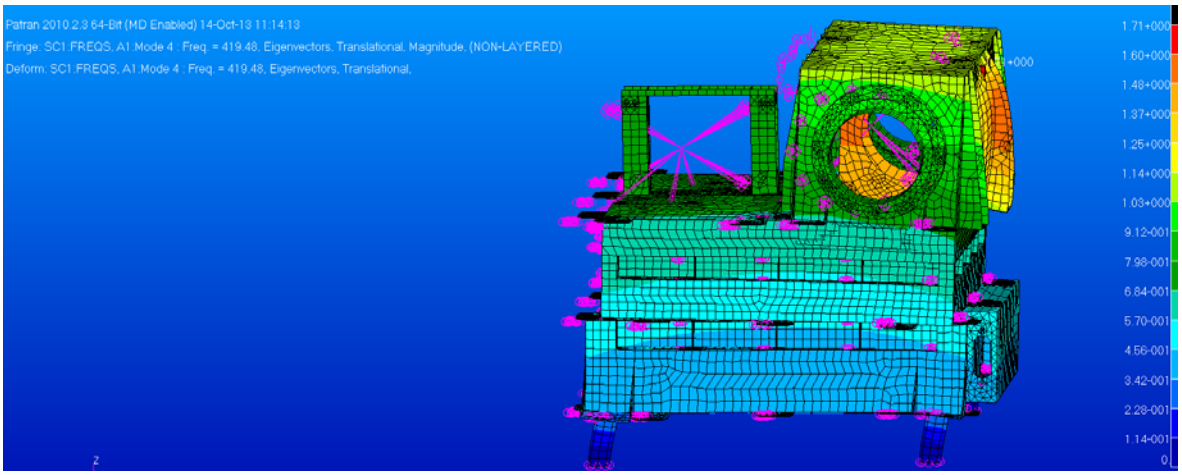

Figure 6-4 Fourth Mode (419 Hz).

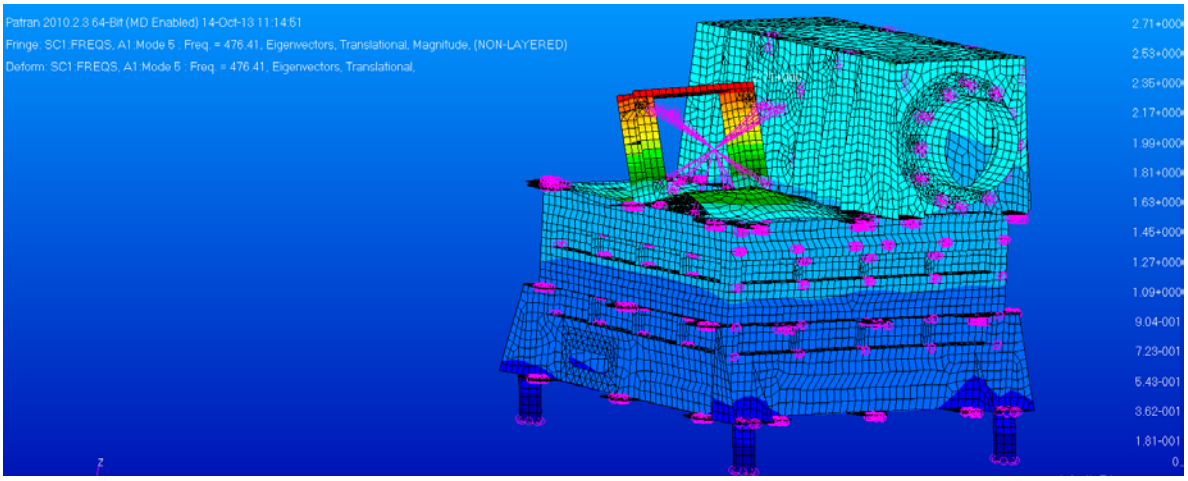

Figure 6-5 Fifth Mode (476 Hz).

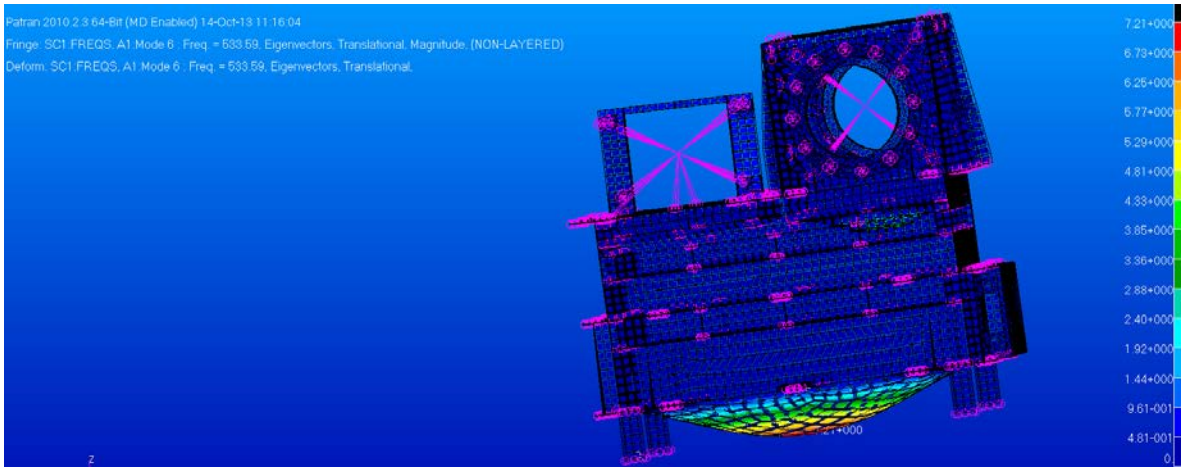

Figure 6-6 Sixth Mode (533 Hz).

The associated modal effective masses are showed in the Table 6-2 and Table 6-3. As it can be appreciated the first three modes appear in the boards.

Mode	Freq.(Hz)	MEM – T1 (x)		MEM – T2 (y)		MEM – T3 (z)	
		(%)	(sum) (%)	(%)	(sum) (%)	(%)	(sum) (%)
1º	348.3	0.00%	0.00%	0.02%	0.02%	14.35%	14.35%
2º	350.4	0.00%	0.00%	0.00%	0.02%	1.35%	15.70%
3º	360.6	0.00%	0.00%	0.00%	0.02%	2.01%	17.71%
4º	419.5	0.03%	0.03%	74.71%	74.73%	0.08%	17.79%
5º	476.4	69.10%	69.13%	0.00%	74.74%	0.05%	17.84%
6º	533.6	0.17%	69.30%	1.58%	76.32%	15.34%	33.18%
7º	542.3	0.09%	69.39%	0.88%	77.20%	1.80%	34.98%
8º	619.0	8.70%	78.09%	0.30%	77.50%	0.04%	35.03%
9º	619.4	15.03%	93.11%	0.00%	77.50%	0.04%	35.06%
10º	647.0	0.03%	93.14%	0.29%	77.79%	0.18%	35.24%
11º	660.8	0.00%	93.14%	0.06%	77.85%	0.00%	35.24%
12º	686.3	0.06%	93.20%	10.24%	88.09%	5.91%	41.15%
13º	725.7	0.03%	93.23%	2.92%	91.02%	4.27%	45.42%
14º	743.4	0.23%	93.46%	0.01%	91.03%	0.06%	45.48%
15º	774.2	0.72%	94.18%	0.00%	91.03%	0.00%	45.48%
16º	801.3	0.11%	94.30%	0.00%	91.03%	0.01%	45.50%
17º	812.5	0.41%	94.71%	0.00%	91.03%	0.01%	45.51%
18º	834.7	0.00%	94.71%	2.24%	93.27%	15.57%	61.08%
19º	866.8	2.06%	96.77%	0.00%	93.27%	0.05%	61.12%
20º	908.2	0.00%	96.77%	0.01%	93.28%	0.18%	61.30%

Table 6-2 Eigenfrequencies and associated modal effective masses – Traslational DoFs.

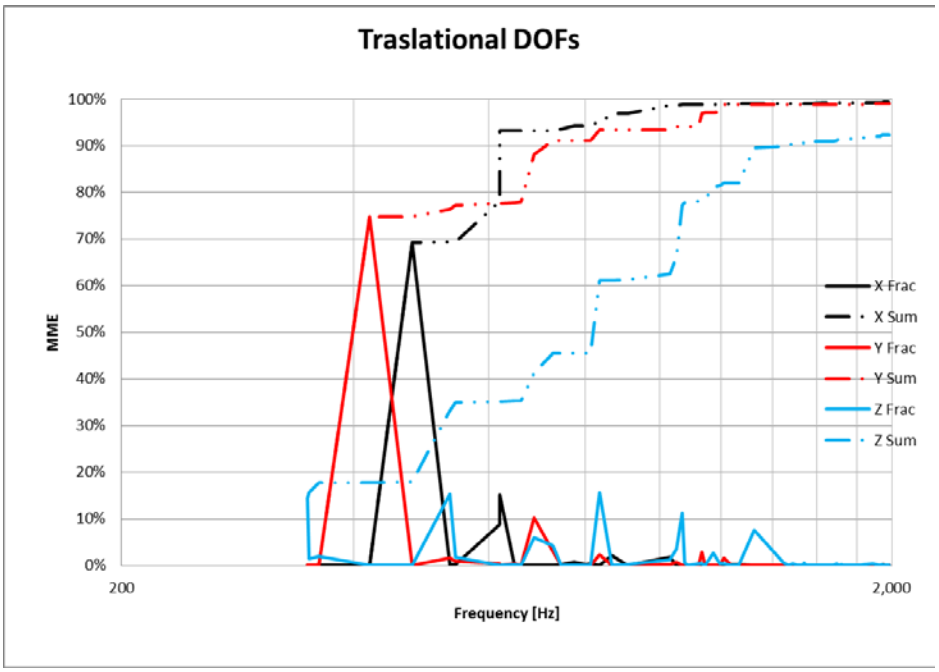

Figure 6-7 Modal effective masses fractional and accumulated – Translational DoFs.

Mode	Freq.(Hz)	MEM – R1		MEM – R2		MEM – R3	
		(%)	(sum) (%)	(%)	(sum) (%)	(%)	(sum) (%)
1º	348.3	0.01%	0.01%	0.00%	0.00%	0.00%	0.00%
2º	350.4	0.00%	0.02%	0.00%	0.00%	0.00%	0.00%
3º	360.6	0.00%	0.02%	0.00%	0.00%	0.00%	0.00%
4º	419.5	73.59%	73.61%	0.04%	0.04%	0.02%	0.02%
5º	476.4	0.00%	73.61%	67.85%	67.89%	0.23%	0.25%
6º	533.6	2.52%	76.13%	0.12%	68.01%	0.00%	0.25%
7º	542.3	1.61%	77.75%	0.07%	68.09%	0.00%	0.25%
8º	619.0	0.40%	78.15%	2.01%	70.10%	5.40%	5.65%
9º	619.4	0.14%	78.29%	6.27%	76.37%	11.38%	17.02%
10º	647.0	0.39%	78.68%	0.01%	76.38%	0.02%	17.04%
11º	660.8	0.34%	79.02%	0.01%	76.39%	0.00%	17.04%
12º	686.3	0.07%	79.09%	0.01%	76.39%	0.19%	17.23%

13º	725.7	0.66%	79.75%	0.01%	76.40%	0.03%	17.26%
14º	743.4	0.05%	79.80%	2.41%	78.81%	0.50%	17.76%
15º	774.2	0.00%	79.80%	2.04%	80.85%	1.17%	18.93%
16º	801.3	0.00%	79.80%	0.89%	81.74%	0.58%	19.51%
17º	812.5	0.00%	79.81%	0.37%	82.12%	0.95%	20.46%
18º	834.7	0.20%	80.00%	0.01%	82.12%	0.06%	20.52%
19º	866.8	0.00%	80.00%	0.35%	82.48%	69.17%	89.68%
20º	908.2	0.01%	80.02%	0.05%	82.53%	0.00%	89.68%

Table 6-3 Eigenfrequencies and associated modal effective masses – Rotational DoFs.

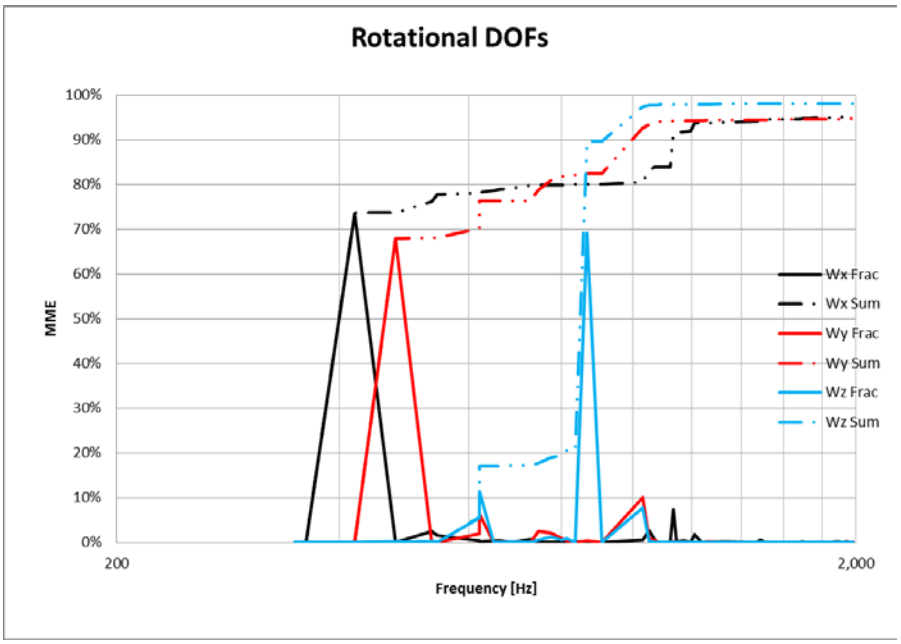

Figure 6-8 Modal effective masses fractional and accumulated – Rotational DoFs.

6.2 Quasi-static analysis

There is no design quasi-static loads specified in the latest version of EID-A [AD1]. The quasi-static load specification included in an older version of EID-A [RD6] has been taken into account.

Stresses caused by quasi-static loads, which are described in RD6, have been analysed. The design loads applicable to EPT-HET is in Table 6-4:

Design Load Factor [g]		
X	Y	Z
69.4	69.4	69.4

Table 6-4 Mass-Acceleration (g).

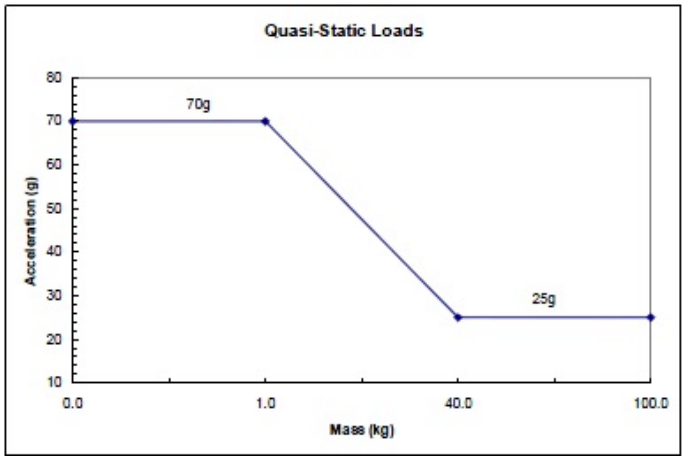

Figure 6-9 Quasi-Static specification.

Nastran solution sequence 101 has been used to perform the analysis. Results (see Table 6-5) show that the stress level is small and far from the materials yield or ultimate levels.

Load Case	Von Mises Maximum Stresses (MPa)			BAR Stresses, Maximum Combined (MPa)
	Al_6061-T6	PCB	Ultem	Ti_6Al_4V
Quasi-static X	42.0	4.2	25.0	208.0
Quasi-static Y	74.2	11.2	32.0	197.0
Quasi-static Z	38.7	28.9	12.4	65.0

Table 6-5 Von Mises Maximum Stresses and BAR Maximum combined Stresses for Quasi-Static analysis.

The stress distribution can be shown in the following figures.

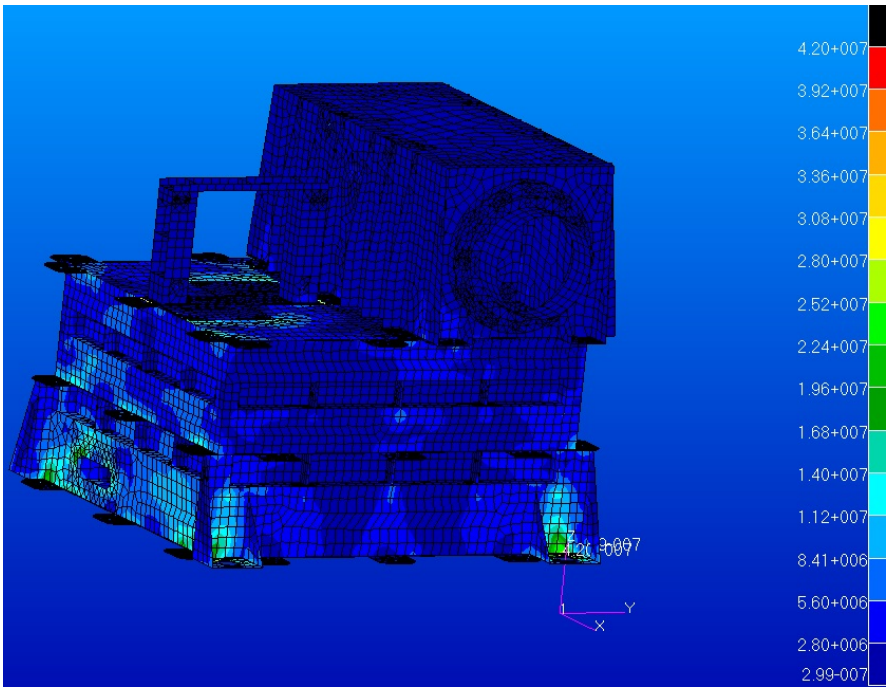

Figure 6-10 Maximum Von Mises stress for Al 6061-T6 structure - Quasi-Static in X.

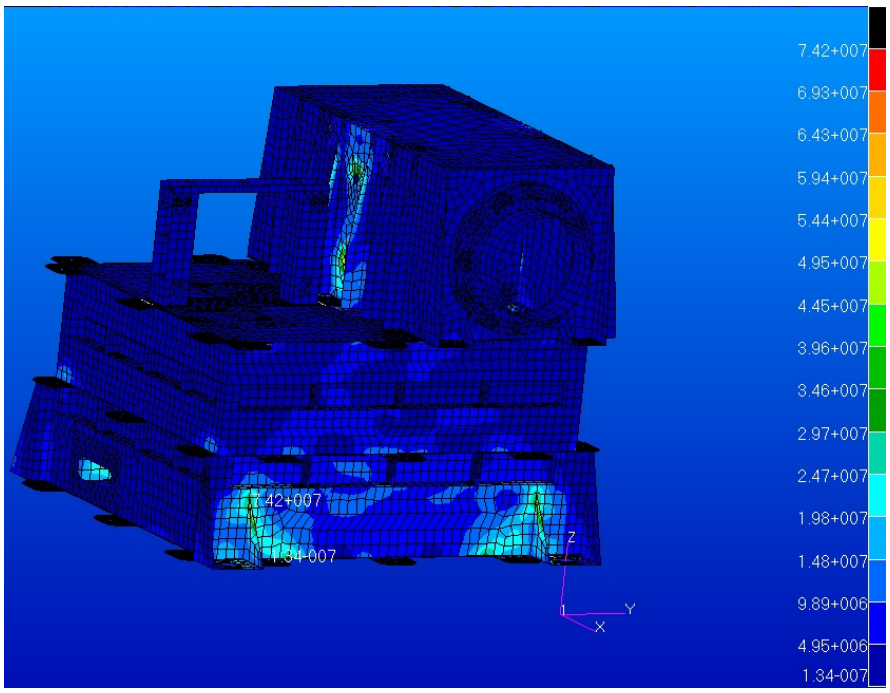

Figure 6-11 Maximum Von Mises stress for Al 6061-T6 structure - Quasi-Static in Y.

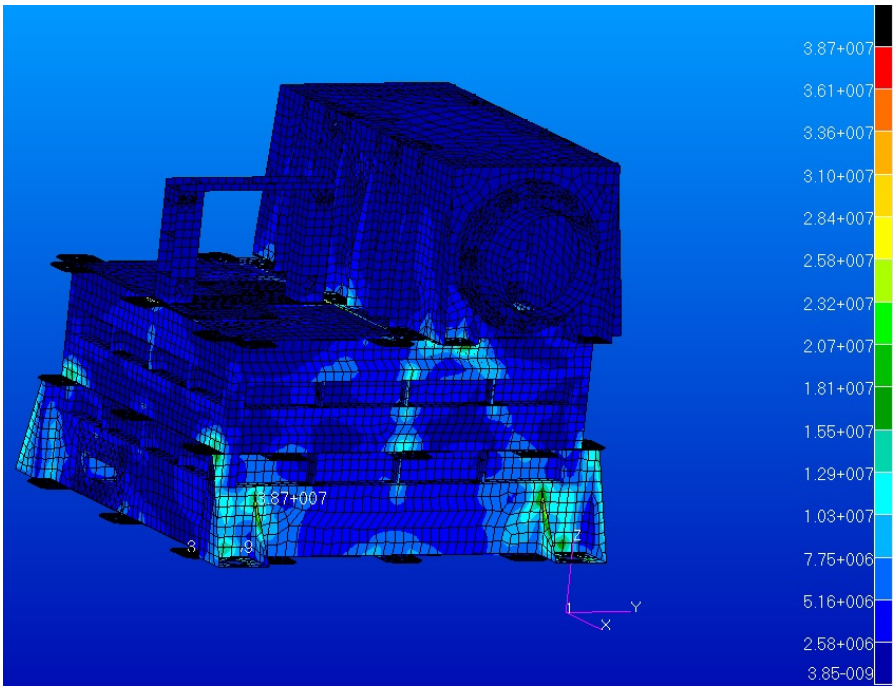

Figure 6-12 Maximum Von Mises stress for Al 6061-T6 structure - Quasi-Static in Z.

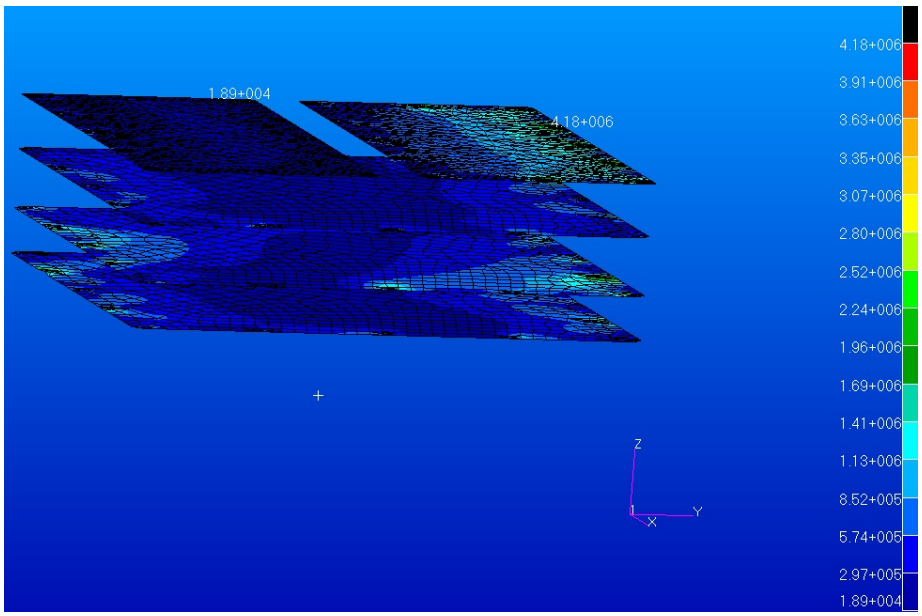

Figure 6-13 Maximum Von Mises stress for PCB - Quasi-Static in X.

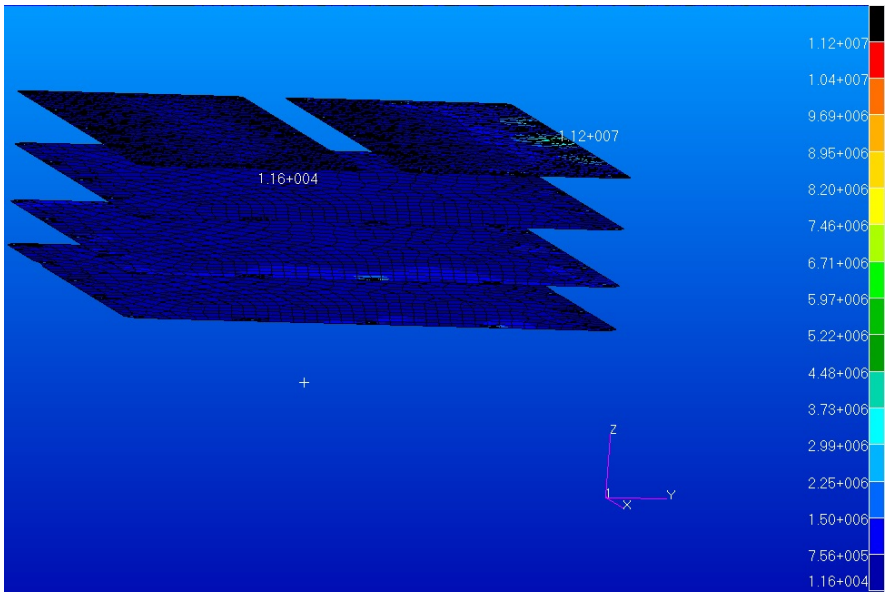

Figure 6-14 Maximum Von Mises stress for PCB - Quasi-Static in Y.

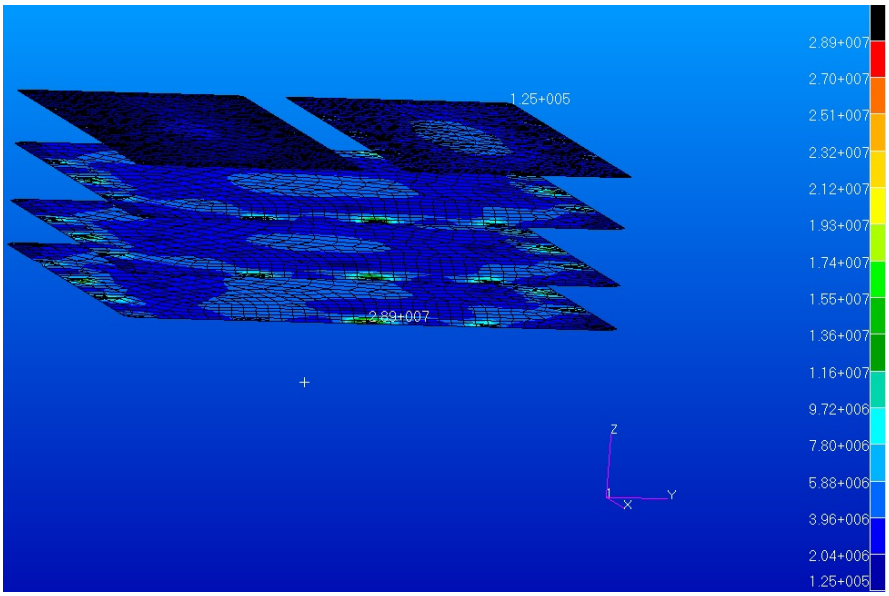

Figure 6-15 Maximum Von Mises stress for PCB - Quasi-Static in Z.

In order to obtain the margins of safety regarding the stresses in the structure, the margins to be applied are the following:

K_P	K_M	K_{LD}	FOSY	FOSU
1.1	1.1	1.1	1.1	1.25

Table 6-6 Safety factors.

The maximum stresses reached in the structure are shown in Table 6-5. The safety factors to be applied will be: $K_P \cdot K_M \cdot K_{LD} \cdot FOSY = 1.46$ for yield strength, and $K_P \cdot K_M \cdot K_{LD} \cdot FOSU = 1.66$ for ultimate strength. For the materials used in the model, the yield tensile strength and the ultimate tensile strength are presented in the Table 4-1. The margins of safety are calculated by the following expressions:

$$MoS_y = \left(\frac{\sigma_Y}{\sigma_{VM\,\max} \times K_p \times K_M \times K_{LD} \times FOSY} \right) - 1 = \left(\frac{\sigma_Y}{\sigma_{VM\,\max} \times 1.1 \times 1.1 \times 1.1 \times 1.1} \right) - 1$$

$$MoS_u = \left(\frac{\sigma_U}{\sigma_{VM\,\max} \times K_p \times K_M \times K_{LD} \times FOSU} \right) - 1 = \left(\frac{\sigma_U}{\sigma_{VM\,\max} \times 1.1 \times 1.1 \times 1.1 \times 1.25} \right) - 1$$

Load Case	Al_6061-T6		PCB		Ultem		Ti_6Al_4V	
	MoSy	MoSu	MoSy	MoSu	MoSy	MoSu	MoSy	MoSu
Quasi-Static X	3.49	3.44	49.41	48.37	3.23	2.97	1.78	1.67
Quasi-Static Y	1.54	1.51	17.90	17.51	2.31	2.10	1.94	1.82
Quasi-Static Z	3.87	3.81	6.33	6.18	7.54	7.00	7.90	7.54

Table 6-7 Margins of Safety for Quasi-Static Analysis.

The SPCs resultant loads can be seen in Table 6-8. They have been obtained recovering the loads with CELAS2 elements (only forces corresponding to translational DoFs have been gathered) and applying safety margins of 20%.

I/F	Node Id..	Quasi-static X		Quasi-static Y		Quasi-static Z	
		In-Plane Load (N)	Axial Load (N)	In-Plane Load (N)	Axial Load (N)	In-Plane Load (N)	Axial Load (N)
1	100000	338.4	298.1	294.4	338.4	320.2	66.8
2	100007	332.8	340.3	354.1	332.8	320.4	75.9
3	100014	338.8	361.0	353.9	338.8	328.7	78.6

4	100021	335.3	302.6	294.5	335.3	329.0	63.7

Table 6-8 Quasi-Static Analysis X, Y, Z – I/F forces.

A combined case analysis has been done, combining as out of plane load 69.4g in Z axis and as in plane load $\sqrt{2}\cdot 69.4$g in the plane XY. The analyses have been done varying the angle of the in-plane load with the X axis every 45º.

Load Case	Design Load X (g)	Design Load Y (g)	Design Load Z (g)
0º	$\sqrt{2}\cdot 69.4$	0	69.4
45º	69.4	69.4	69.4
90º	0	$\sqrt{2}\cdot 69.4$	69.4
135º	-69.4	69.4	69.4
180º	$-\sqrt{2}\cdot 69.4$	0	69.4
225º	-69.4	-69.4	69.4
270º	0	$-\sqrt{2}\cdot 69.4$	69.4
315º	69.4	-69.4	69.4

Table 6-9 Mass acceleration (g).

The maximum Von Mises stresses and the BAR stresses (maximum combined) are presented in Table 6-10.

In plane load angle with X axis [deg]	Von Mises Maximum Stresses (MPa)			BAR Stresses, Maximum Combined (MPa)
	Al_6061-T6	PCB	Ultem	Ti_6Al_4V
0º	62.0	29.0	42.1	334.0
45º	114.0	29.0	50.6	258.0
90º	144.0	29.4	49.9	293.0
135º	112.0	29.8	44.4	260.0
180º	68.5	29.7	38.2	318.0

225º	106.0	29.2	57.5	288.0
270º	121.0	32.9	57.4	301.0
315º	96.2	29.0	46.1	296.0

Table 6-10 Von Mises Maximum Stresses and BAR Maximum combined Stresses.

In order to obtain the margins of safety regarding the stresses in the structure, the margins applied are the indicated in Table 6-6.

The maximum stresses reached in the structure are shown in Table 6-10. The safety factors to be applied will be: $K_P \cdot K_M \cdot K_{LD} \cdot FOSY = 1.46$ for yield strength, and $K_P \cdot K_M \cdot K_{LD} \cdot FOSU = 1.66$ for ultimate strength. For the materials used in the model, the yield tensile strength and the ultimate tensile strength are presented in the Table 4-1.The margins of safety are calculated are:

In plane load angle with X axis [deg]	Al_6061-T6		PCB		Ultem		Ti_6Al_4V	
	MoSy	MoSu	MoSy	MoSu	MoSy	MoSu	MoSy	MoSu
0º	2.04	2.01	6.30	6.15	1.51	1.36	0.73	0.66
45º	0.65	0.63	6.30	6.15	1.09	0.96	1.24	1.15
90º	0.31	0.29	6.20	6.05	1.12	0.99	0.97	0.90
135º	0.68	0.66	6.11	5.96	1.38	1.23	1.23	1.14
180º	1.75	1.72	6.13	5.98	1.77	1.60	0.82	0.75
225º	0.78	0.76	6.25	6.10	0.84	0.72	1.01	0.93
270º	0.56	0.54	5.44	5.30	0.84	0.73	0.92	0.85
315º	0.96	0.94	6.30	6.15	1.30	1.15	0.95	0.88

Table 6-11 Margins of Safety for Combined Quasi-Static Analysis.

The SPCs resultant loads can be seen in Table 6-12. They have been obtained recovering the loads with CELAS2 elements (only forces corresponding to translational DoFs have been gathered) and applying safety margins of 20%.

In plane load angle with X axis (deg)	Node: 100000		Node: 100007		Node: 100014		Node: 100021	
	In-Plane Load (N)	Axial Load (N)	In-Plane Load (N)	Axial Load (N)	In-Plane Load (N)	Axial Load (N)	In-Plane Load (N)	Axial Load (N)
0º	354.9	126.2	405.8	143.4	588.9	877.2	491.5	692.6
45º	574.5	903.6	469.1	390.4	476.0	305.8	341.6	310.3
90º	506.3	742.9	454.1	95.9	464.7	88.3	493.9	741.4
135º	575.5	904.6	470.1	390.9	476.4	306.0	341.6	310.7
180º	488.4	706.3	557.0	858.0	432.2	123.9	364.4	140.3
225º	405.0	264.2	588.7	1031.8	403.0	351.4	471.6	347.3
270º	458.9	162.7	498.3	810.5	505.4	841.5	462.3	189.0
315º	468.3	324.5	384.5	323.7	606.6	1059.3	415.1	241.7

Table 6-12 Combined Quasi-Static resultant loads – I/F Forces.

6.3 Sine Vibration Analysis

According to EID-A Requirement (**EIDA i4 R-497**) [AD1], a sine vibration analysis has been carried on. The qualification level for sine vibration test can be seen in Table 6-13 and Figure 6-16.

Axis	Frequency (Hz)	Qualification
Out of Plane	5-20	15 mm
	20-100	24 g
In Plane	5-20	9.9 mm
	20-100	16 g
		2 Oct/min

Table 6-13 Sine Vibration test levels – EPT/HET.

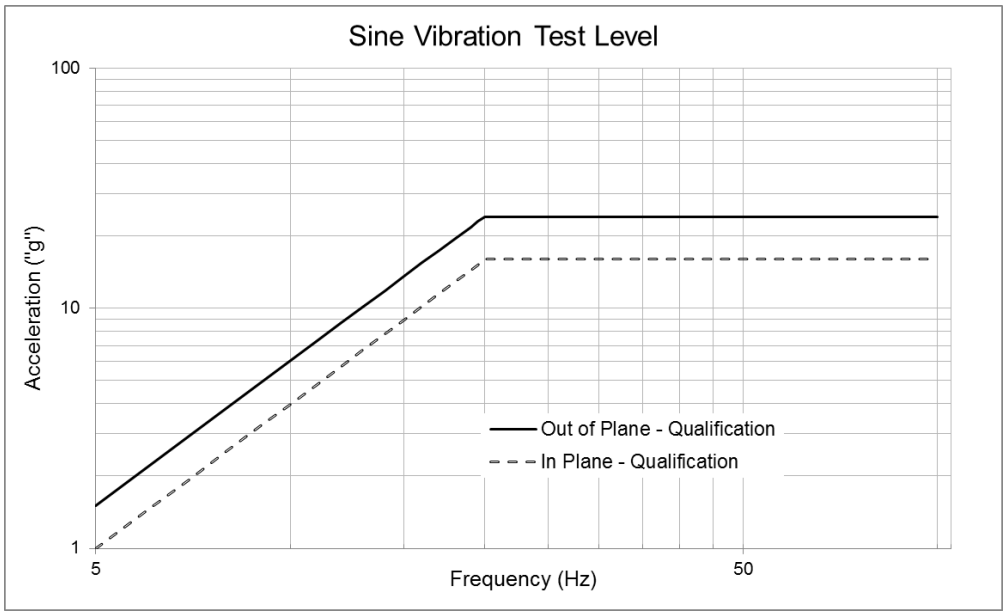

Figure 6-16 Sine Vibration test levels – EPT/HET.

As the first eigenfrequency (348 Hz) is far away from the highest frequency for the sine vibration test level (100 Hz), the acceleration frequency response is almost the same as the input. Regarding the forces at the interfaces, their values have been recovered with CELAS2 elements, and they have been gathered in Table 6-14. The maximum values correspond to a frequency value equal to 100 Hz. There are no margins applied on the forces values. The structural damping of the model in the sine analysis was 2.5%.

I/F	Node Id.	Sine Vibration – X axis		Sine Vibration – Y axis		Sine Vibration – Z axis	
		In-Plane Load (N)	Axial Load (N)	In-Plane Load (N)	Axial Load (N)	In-Plane Load (N)	Axial Load (N)
1	100000	69	66	60	60	20	86
2	100007	68	66	69	72	23	106
3	100014	69	68	73	72	24	113
4	100021	69	68	61	60	19	84

Table 6-14 Sine Vibration analysis – I/F Forces.

Regarding the stresses resulting from the sine vibration analysis, the maximum values obtained have been gathered in Table 6-15.

Load Case	Von Mises Maximum Stresses (MPa)			Von Mises Maximum BAR Stresses (MPa)
	Al_6061-T6	PCB	Ultem	Ti_6Al_4V
Sine Vibration X axis (f = 100 Hz)	9.0	1.0	5.3	50.4
Sine Vibration Y axis (f = 100 Hz)	14.9	2.3	7.1	49.0
Sine Vibration Z axis (f = 100 Hz)	11.0	10.9	3.9	23.5

Table 6-15 Sine Vibration analysis – Maximum stresses.

The stress distribution can be shown in the following figures.

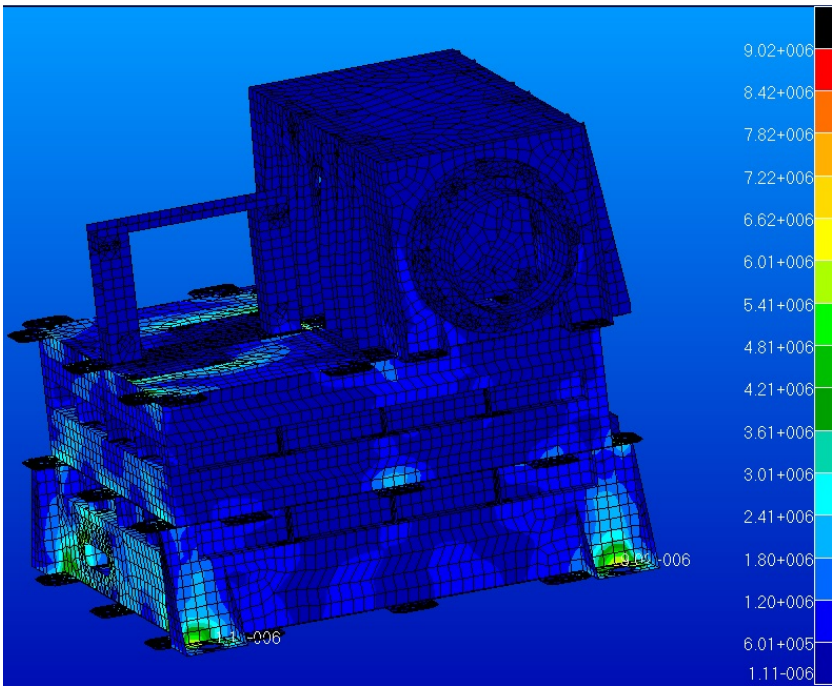

Figure 6-17 Maximum Von Mises stress for Al 6061-T6 structure – Sine Vibration in X.

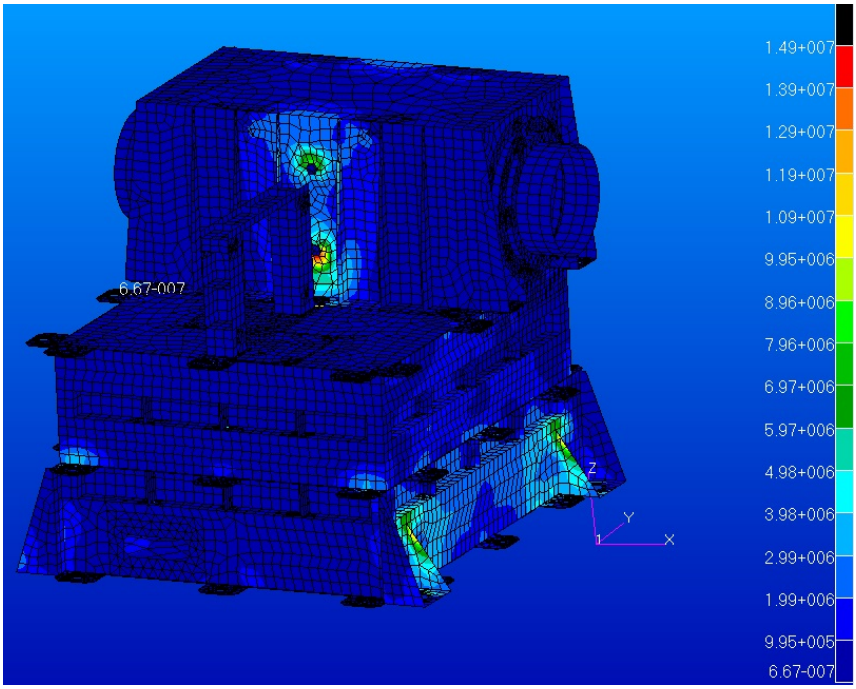

Figure 6-18 Maximum Von Mises stress for Al 6061-T6 structure – Sine Vibration in Y.

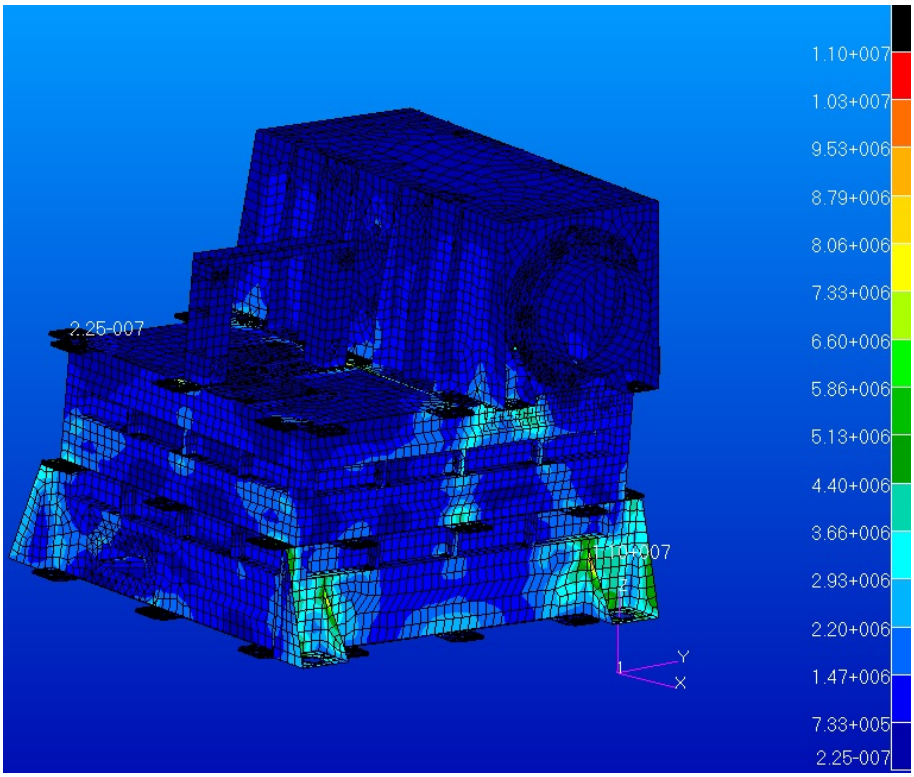

Figure 6-19 Maximum Von Mises stress for Al 6061-T6 structure – Sine Vibration in Z.

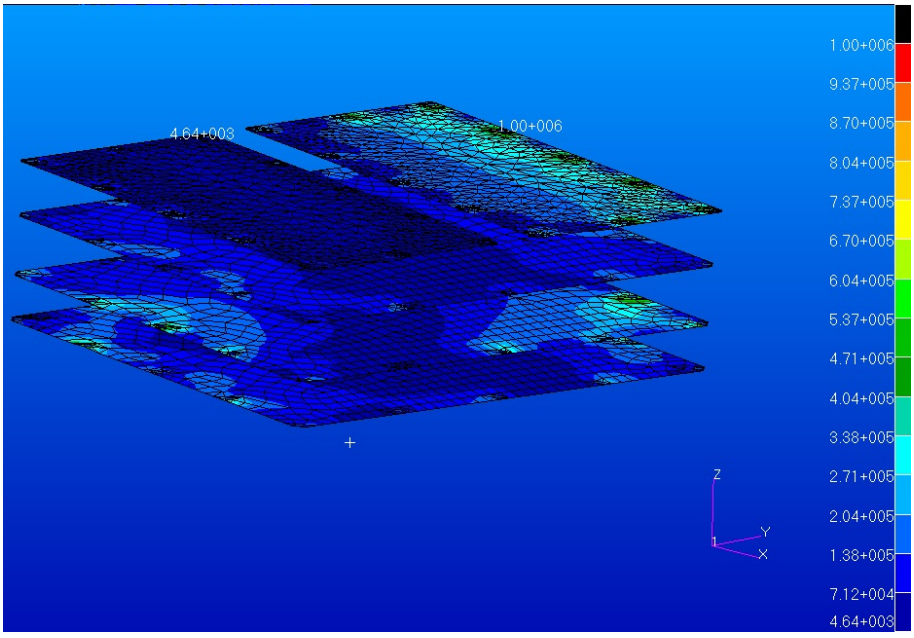

Figure 6-20 Maximum Von Mises stress for PCB – Sine Vibration in X.

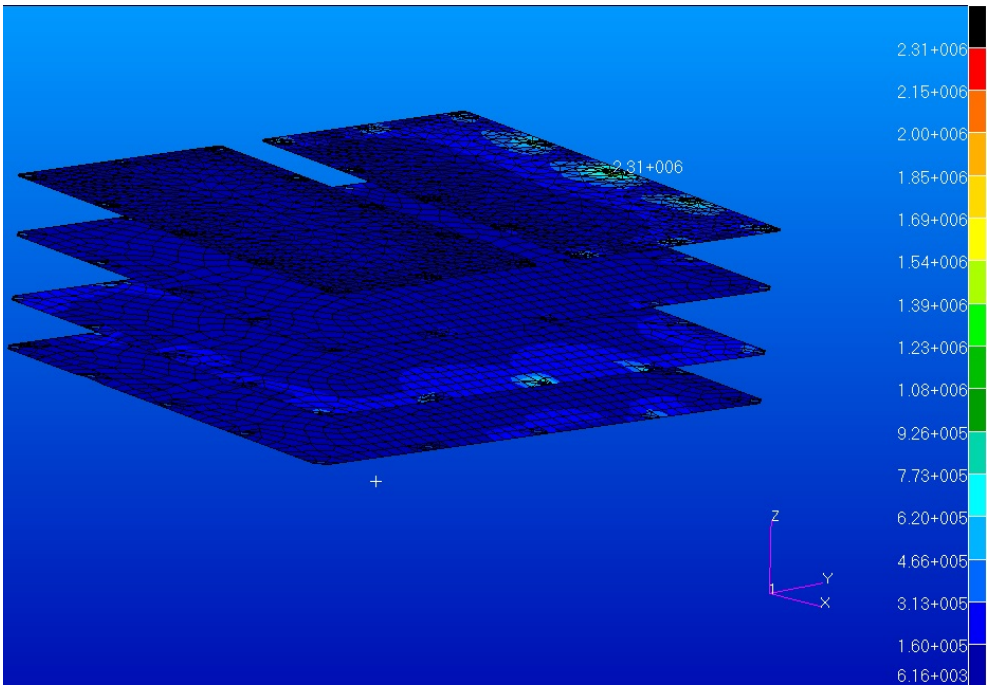

Figure 6-21 Maximum Von Mises stress for PCB – Sine Vibration in Y.

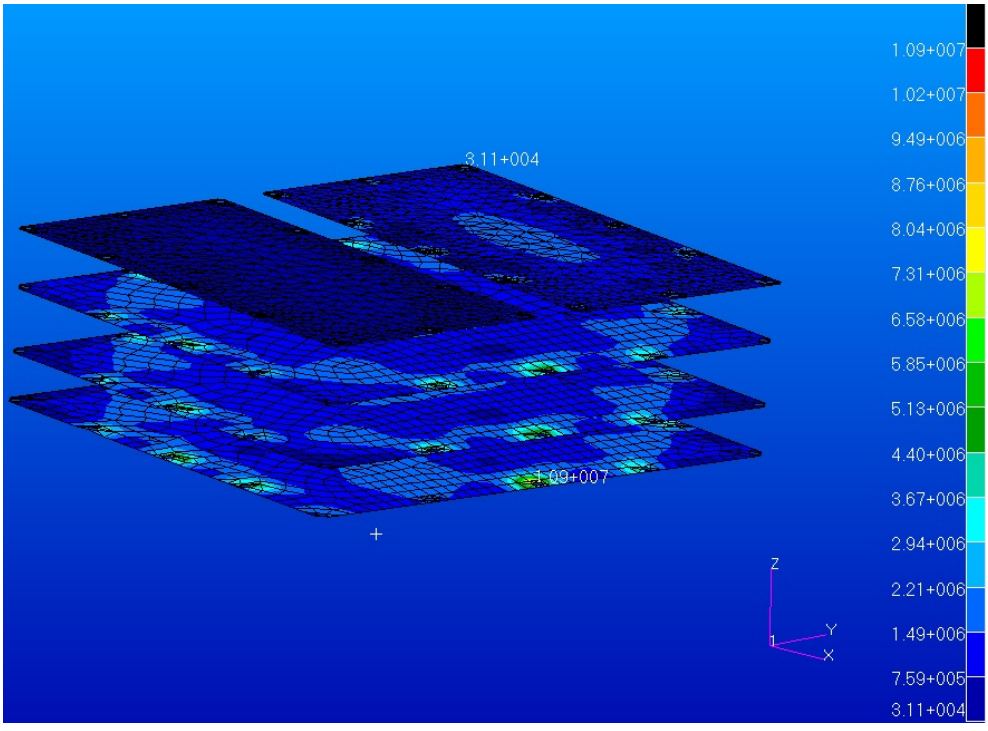

Figure 6-22 Maximum Von Mises stress for PCB – Sine Vibration in Z.

In order to obtain the margins of safety regarding the stresses in the structure, the margins applied are the indicated in Table 6-6.

The maximum stress reached in the structure is shown in Table 6-15. The total margins to be applied will be: $K_P \cdot K_M \cdot K_{LD} \cdot FOSY = 1.46$ for yield strength and $K_P \cdot K_M \cdot K_{LD} \cdot FOSU = 1.66$ for ultimate strength. For the materials used in the model, the yield tensile strength and the ultimate tensile strength are presented in the Table 4-1.The margins of safety calculated are:

Load Case	Al_6061-T6		PCB		Ultem		Ti_6Al_4V	
	MoSy	MoSu	MoSy	MoSu	MoSy	MoSu	MoSy	MoSu
Sine Vibration X axis (f = 100 Hz)	19.95	19.70	210.73	206.36	18.97	17.71	10.48	10.02
Sine Vibration Y axis (f = 100 Hz)	11.65	11.51	91.06	89.16	13.91	12.97	10.81	10.33
Sine Vibration Z axis (f = 100 Hz)	16.14	15.94	18.43	18.02	26.15	24.43	23.62	22.63

Table 6-16 Margins of Safety for Sine Vibration Analysis.

6.4 Random Vibration Analysis

According to STM vibration test report [RD4], a random vibration analysis has been carried on. The qualification level for random vibration test can be seen in Table 6-17 and Figure 6-23.

Axis / unit mass	Frequency (Hz)	Qualification
Perpendicular to mounting plane 0.5 kg <Mass < 3 kg (1 axis)	20-100	+12 dB/Oct
	100-500	1 g^2/Hz
	500-2000	−8 dB/Oct
		26.3 g rms
Parallel to mounting plane All Unit Masses	20-80	+4 dB/Oct
	80-1000	0.1 g^2/Hz
	1000-2000	−3 dB/Oct
		12.8 g rms

Table 6-17 Random Vibration test levels – EPT/HET.

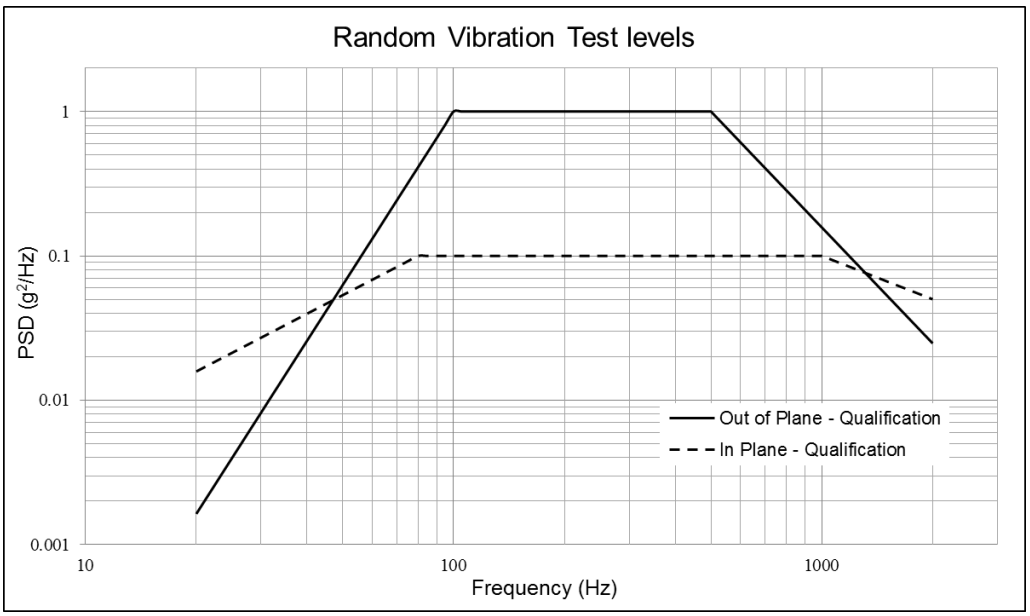

Figure 6-23 Random Vibration test levels – EPT/HET.

The forces at the interfaces have been recovered with CELAS2 elements. The RMS values have been gathered in Table 6-18. The structural damping of the model in the random analysis was 2.5%.

Point ID.	Random Vibration X axis resultant forces		Random Vibration Y axis resultant forces		Random Vibration Z axis resultant forces	
	In-Plane Load (N)	Axial Load (N)	In-Plane Load (N)	Axial Load (N)	In-Plane Load (N)	Axial Load (N)
100000	118	147	109	133	54	135
100007	115	148	124	156	61	186
100014	116	148	130	152	71	212
100021	118	157	108	127	57	134

Table 6-18 Random Vibration analysis – I/F RMS Forces.

Regarding the stresses resulting from the random vibration analysis, the maximum values obtained with 3 times RMS have been gathered in Table 6-19.

Load Case	Von Mises Maximum (3 x RMS) Stresses (MPa)			Maximum Combined BAR Stresses (3 x RMS) (MPa)
	Al_6061-T6	PCB	Ultem	Ti_6Al_4V
Random vibration X axis	109.0	12.7	28.6	246.0
Random Vibration Y axis	166.0	36.9	38.5	229.0
Random Vibration Z axis	137.0	103.0	26.7	119.0

Table 6-19 Random Vibration analysis – Maximum stresses in the structure.

The stress distribution can be shown in the following figures.

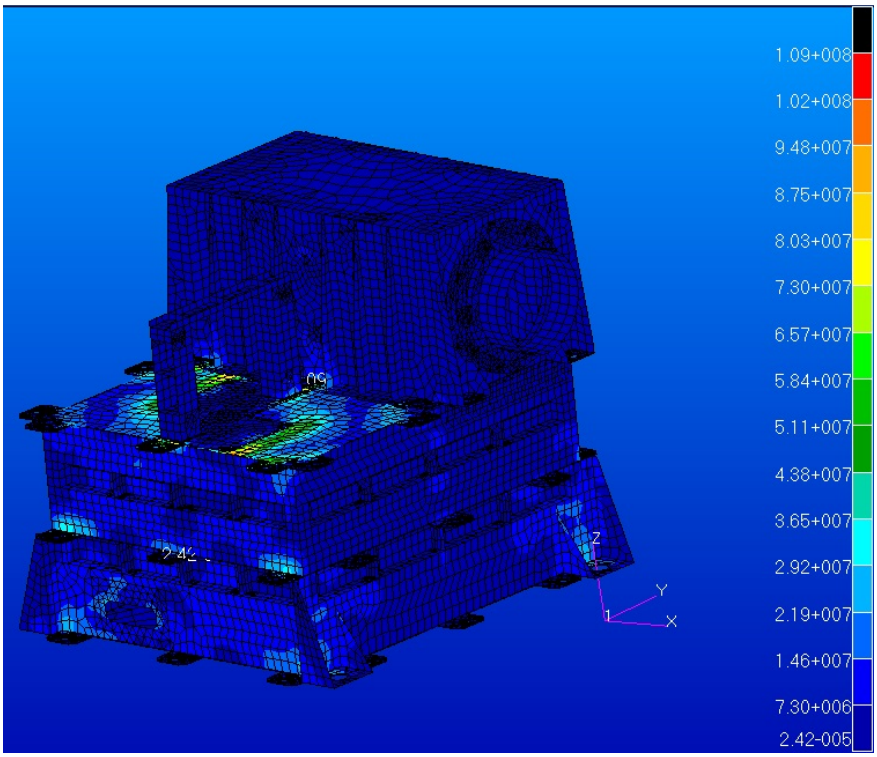

Figure 6-24 Maximum Von Mises (3 x RMS) stress for Al 6061-T6 structure – Random Vibration in X.

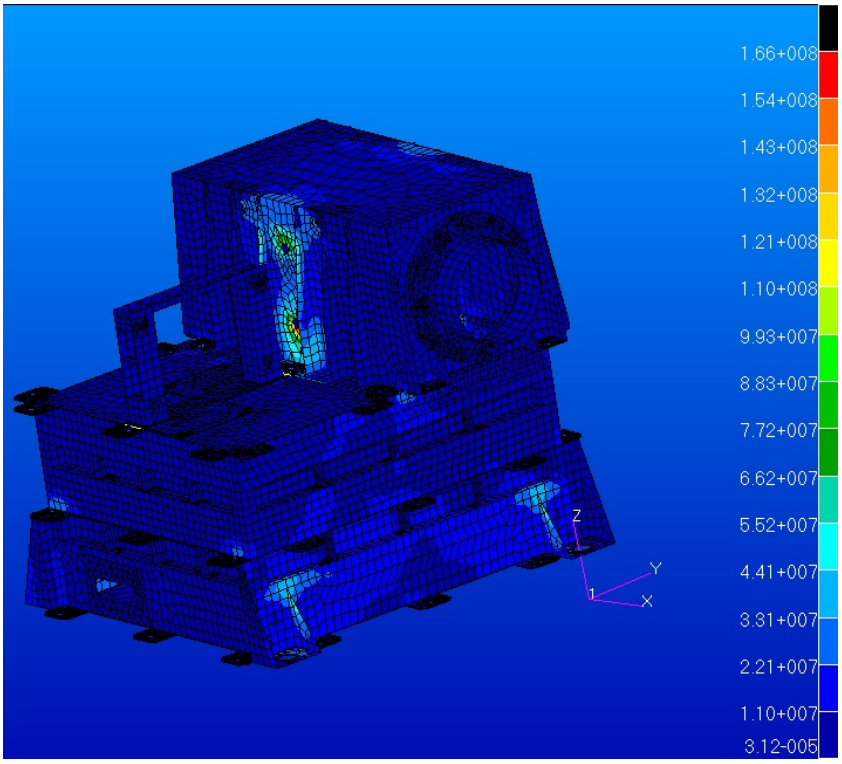

Figure 6-25 Maximum Von Mises (3 x RMS) stress for Al 6061-T6 structure – Random Vibration in Y.

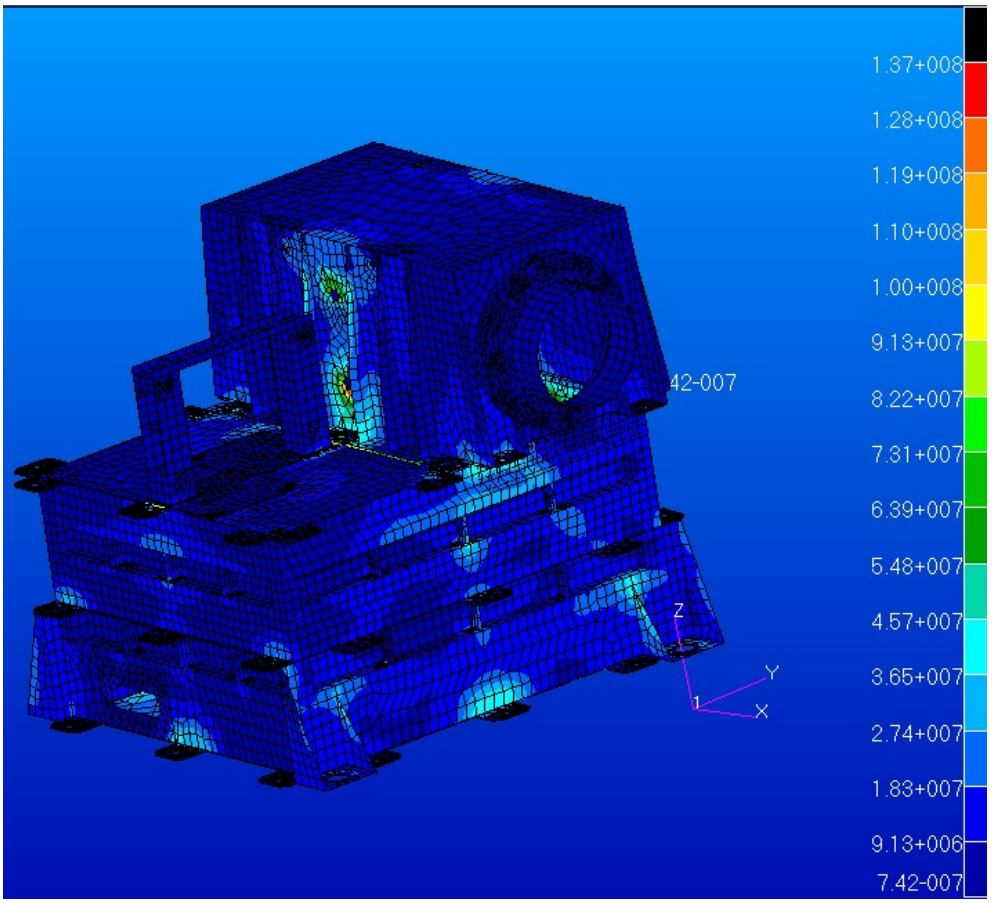

Figure 6-26 Maximum Von Mises (3 x RMS) stress for Al 6061-T6 structure – Random Vibration in Z.

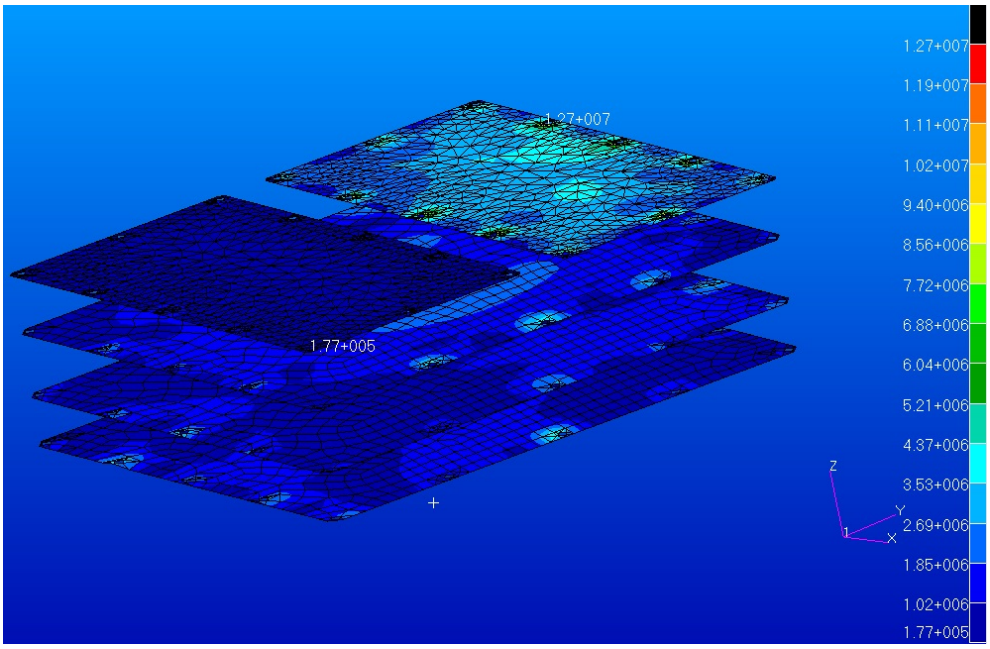

Figure 6-27 Maximum Von Mises (3 x RMS) stress for PCB – Random Vibration in X.

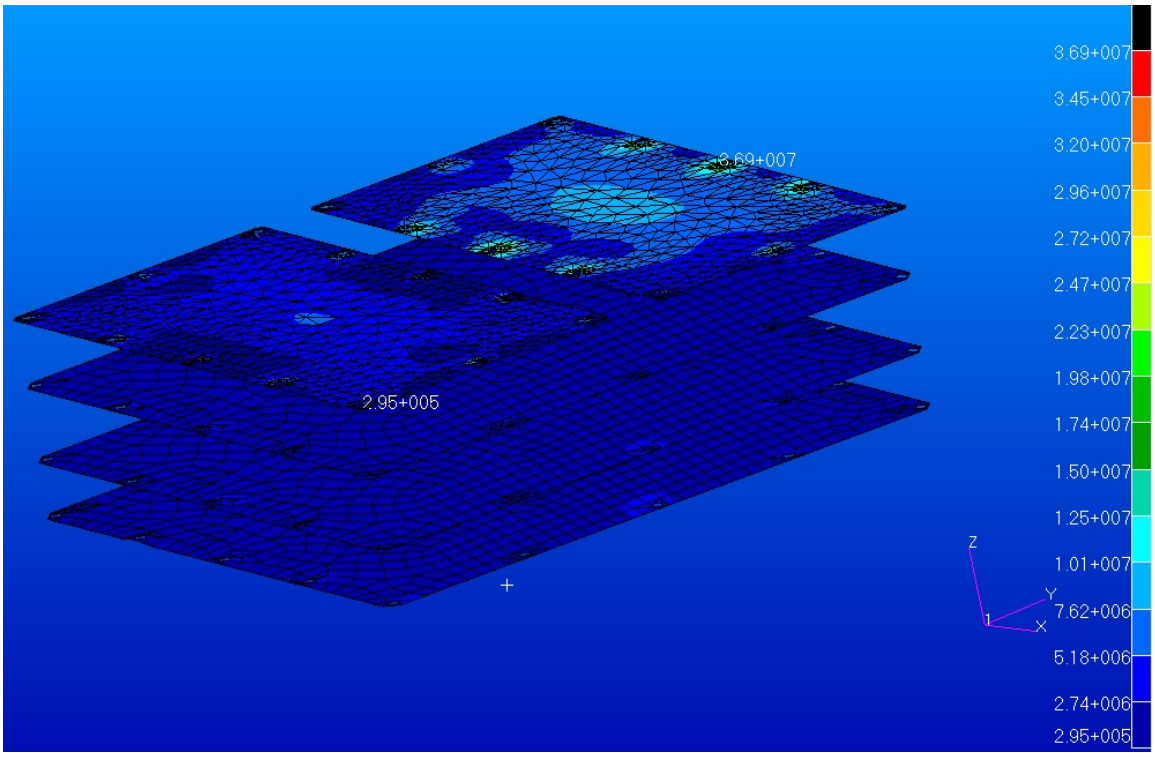

Figure 6-28 Maximum Von Mises (3 x RMS) stress for PCB – Random Vibration in Y.

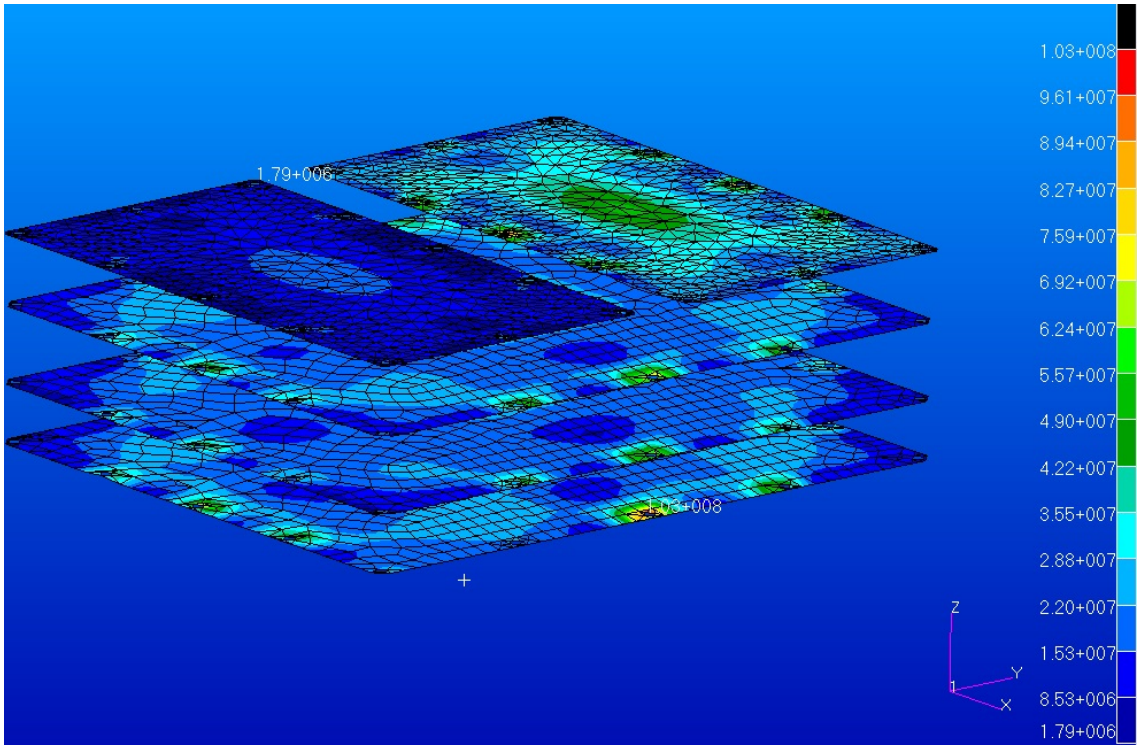

Figure 6-29 Maximum Von Mises (3 x RMS) stress for PCB – Random Vibration in Z.

In order to obtain the margins of safety regarding the stresses in the structure the margins applied are indicated in Table 6-6.

The maximum stresses reached in the structure is shown in Table 6-19. The total margins to be applied will be: $K_P \cdot K_M \cdot K_{LD} \cdot FOSY = 1.46$ for yield strength and $K_P \cdot K_M \cdot K_{LD} \cdot FOSU = 1.66$ for ultimate strength. For the materials used in the model, the yield tensile strength and the ultimate tensile strength are presented in the Table 4-1. The margins of safety calculated are:

Load Case	Al_6061-T6		PCB		Ultem		Ti_6Al_4V	
	MoSy	MoSu	MoSy	MoSu	MoSy	MoSu	MoSy	MoSu
Random Vibration X axis	0.73	0.71	15.67	15.33	2.70	2.47	1.35	1.26
Random Vibration Y axis	0.14	0.12	4.74	4.62	1.75	1.58	1.53	1.43
Random Vibration Z axis	0.38	0.36	1.06	1.01	2.97	2.71	3.86	3.67

Table 6-20 Margins of Safety for Random Vibration Analysis.

6.5 Bolt Analysis

For this analysis, the loads from the combined quasi-static analysis have been used (see section 6.2) because it's the most severe load case. The worst conditions of the combined quasi-static analysis cases have been used for each bolt analysis. All load values have been multiplied by the "model factor" K_M, which has been taken equal to 1.2. The final results are shown in Table 6-21.

I/F Point ID.	Load Case	In-Plane (N)	Out of Plane (N)
100000	Quasi-Static 135º	575.5	904.6
100007	Quasi-Static 225º	588.7	1031.8
100014	Quasi-Static 315º	606.6	1059.3
100021	Quasi-Static 90º	493.9	741.4

Table 6-21 Worst conditions of the combined Quasi-Static cases - I/F loads.

6.5.1 Margin of safety on tensile failure

$$MoS_{tot,y} = \frac{A_s \sigma_y}{F_{V,\max} + \varphi F_A s f_y} - 1$$

$$MoS_{tot,ult} = \frac{A_s \sigma_{ult}}{F_{V,\max} + \varphi F_A sf_{ult}} - 1$$

In the above expressions, the following parameters were used:

- Stress area for the fastener (M5) $\equiv A_S = 1.42 \cdot 10^{-5}\ \mathrm{m}^2$
- Yield stress for Ti 6Al 4V $\equiv\ \sigma_y = 847\ \mathrm{MPa}$
- Ultimate stress for Ti 6Al 4V $\equiv\ \sigma_{ult} = 924\ \mathrm{MPa}$
- Maximal guaranteed screw preload $\equiv F_{V,max} = 7400\ \mathrm{N}$
- Force ratio $\equiv \varphi = 0.255$
- Yield safety factor $\equiv sf_y = 1.1$
- Ultimate safety factor $\equiv sf_{ult} = 1.4$
- Axial load (K_M included) $\equiv F_A$

I/F Point ID.	Load Case	Yield MOS	Ultimate MOS
100000	Quasi-Static 135º	0.56	0.69
100007	Quasi-Static 225º	0.56	0.68
100014	Quasi-Static 315º	0.55	0.68
100021	Quasi-Static 90º	0.57	0.70

Table 6-22 Margins of Safety on bolt tensile failure.

6.5.2 No gapping criteria

$$MoS_g = \frac{F_{V,\min}}{(1 - n\varphi) F_A sf_g} - 1$$

For this last expression for the margin of safety, the following parameters are defined additionally to those from previous subsection:

- Minimum guaranteed screw preload $\equiv F_{V,min} = 6500\ \mathrm{N}$
- Gapping safety factor $\equiv sf_g = 1.4$
- Loading plane factor $\equiv n = 0.5$

I/F Point ID.	Load Case	Gapping MOS
100000	Quasi-Static 135º	4.88
100007	Quasi-Static 225º	4.16
100014	Quasi-Static 315º	4.02
100021	Quasi-Static 90º	6.18

Table 6-23 Margins of Safety on gapping.

6.5.3 No sliding criteria

$$MoS_{slip} = \frac{(F_{V,\min} - (1 - n\varphi)F_A)N\mu_s}{F_s sf_{ult}} - 1$$

For this last expression for the margin of safety, the following parameters are defined additionally to those from previous subsections:

- Number of bolts of each joint $\equiv N = 1$
- Friction coefficient $\equiv \mu_s = 0.15$
- Total in plane load of the foot (K_M included) $\equiv F_S$
- Axial load (K_M included) $\equiv F_A$
- Ultimate safety factor $\equiv sf_{ult} = 1.4$

I/F Point ID.	Load Case	Sliding MOS
100000	Quasi-Static 135º	0.06
100007	Quasi-Static 225º	0.02
100014	Quasi-Static 315º	-0.02
100021	Quasi-Static 90º	0.27

Table 6-24 Margins of Safety on sliding.

6.5.4 Margin of safety on fastener shear failure

In those joints in which the no sliding or gaping criteria is not met, margins of safety for both pure shear and combined shear and axial loads have been calculated. As all feet suffer from sliding, the margins were calculated for every bolt.

The expressions for the calculation have been the following:

- Pure shear

$$MoS_{S,y} = \frac{\tau_y A_s}{F_S s f_y} - 1$$

$$MoS_{S,ult} = \frac{\tau_{ult} A_s}{F_S s f_{ult}} - 1$$

- Combined shear and axial loads

$$MoS_{comb,y} = \frac{1}{\left(\frac{F_S s f_y}{\tau_y A_s}\right)^3 + \left(\frac{F_{V,max} + \varphi F_A s f_y}{A_S \sigma_y}\right)^2} - 1$$

$$MoS_{comb,ult} = \frac{1}{\left(\frac{F_S s f_{ult}}{\tau_{ult} A_s}\right)^3 + \left(\frac{F_{V,max} + \varphi F_A s f_{ult}}{A_S \sigma_{ult}}\right)^2} - 1$$

For the expresions for the margins of safety additionally to those from previous subsections, the following parameters are defined:

- Yield shear strength $\equiv \tau_y = 491\ MPa$
- Ultimate shear strength $\equiv \tau_{ult} = 693\ MPa$
- In plane load (KM include) $\equiv F_S$

I/F Point ID.	Load Case	Pure shear		Combined shear	
		Yield MOS	Ultimate MOS	Yield MOS	Ultimate MOS
100014	Quasi-Static 315º	9.44	11.96	1.43	1.86

Table 6-25 Margin of safety on fastener shear failure.

6.6 Standoff crush analysis

This analysis has been done considering the maximum preload and the maximum axial load to verify that the I/F standoffs withstand the most severe crush conditions.

A buckling analysis has been carried out to determine the buckling limit load of standoffs (F_{buck}). For this model, the standoff dimensions are:

- Length = 0.015 m.
- Radius = 0.00413 m.
- Thickness = 0.00275 m.

The standoff buckling limit load is 14394 N.

The margin of safety on standoff crushing are calculated with the following equation:

$$MoS_{crush,y} = \frac{F_{buck}}{F_{V,max} + (1 - \Phi_n)F_A sf_y} - 1$$

For this expression for the margin of safety, the following parameters are defined:

- Buckling limit load $\equiv F_{Buck}$
- Axial load (K_M included) $\equiv F_A$
- Maximal guaranteed screw preload $\equiv F_{V,max} = 7400$ N
- Force ratio of Ultem standoff $\equiv \Phi_n = 0.418$
- Yield safety factor $\equiv sf_y = 1.1$

I/F	Load Case	Axial Load (N)	Crushing MOS
100014	Quasi-Static 315º	1059.3	0.8

Table 6-26 Margin of Safety on Standoff crushing – Minimum value

7 FAIL-SAFE ANALYSIS

This analysis is done by supposing that the most loaded bolt breaks, this is I/F 3 (SPC Node 100014). A modal analysis and a quasi-static analysis are done.

7.1 Normal mode analysis

A normal modes analysis of the model without the bolt interface 3 was performed. The first modes are shown and some figures of them are depicted below. The first eigenfrequency has a value of 276.3 Hz, which is compliant with EID-A requirement (**EIDA R-089**) [AD1], which is that all fundamental resonance frequencies of the instrument should be above 140 Hz.

Mode	Freq.(Hz)	MEM – T1 (x)		MEM – T2 (y)		MEM – T3 (z)	
		(%)	(sum) (%)	(%)	(sum) (%)	(%)	(sum) (%)
1º	276.3	27.44%	27.44%	25.24%	25.24%	19.89%	19.89%
2º	349.9	0.18%	27.62%	1.01%	26.25%	1.26%	21.14%
3º	351.9	1.32%	28.94%	4.54%	30.79%	7.85%	29.00%
4º	361.2	0.33%	29.27%	1.42%	32.21%	2.43%	31.43%
5º	395.2	37.58%	66.85%	45.67%	77.88%	0.29%	31.72%
6º	513.3	8.77%	75.62%	0.34%	78.22%	21.27%	52.99%
7º	540.6	0.03%	75.65%	0.01%	78.23%	0.01%	53.00%
8º	564.3	0.28%	75.93%	0.16%	78.39%	0.16%	53.16%
9º	616.9	1.45%	77.39%	1.03%	79.42%	0.00%	53.16%
10º	645.0	1.18%	78.57%	1.53%	80.95%	0.00%	53.16%
11º	658.2	2.15%	80.72%	0.01%	80.96%	3.14%	56.30%
12º	660.9	0.01%	80.73%	2.99%	83.95%	2.46%	58.76%
13º	678.2	12.86%	93.59%	7.74%	91.69%	5.72%	64.48%
14º	726.5	0.56%	94.15%	0.02%	91.71%	2.83%	67.31%
15º	748.6	0.87%	95.02%	0.12%	91.83%	0.67%	67.97%
16º	782.1	0.85%	95.87%	0.14%	91.97%	2.30%	70.27%
17º	802.1	0.46%	96.34%	0.01%	91.98%	0.77%	71.04%

18º	811.9	0.06%	96.40%	0.01%	91.99%	0.53%	71.57%
19º	833.5	2.30%	98.69%	3.78%	95.77%	6.76%	78.33%
20º	874.2	0.20%	98.90%	0.55%	96.31%	0.35%	78.68%

Table 7-1 Eigenfrequencies and associated modal effective masses – Traslational DoFs.

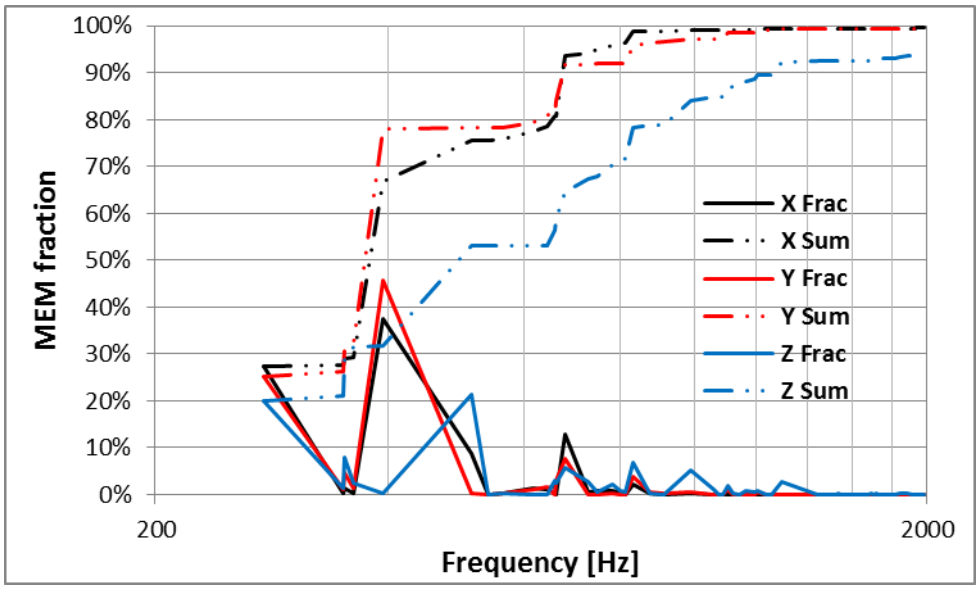

Figure 7-1 Modal effective masses fractional and accumulated – Translational DoF.

Mode	Freq.(Hz)	MEM – R1		MEM – R2		MEM – R3	
		(%)	(sum) (%)	(%)	(sum) (%)	(%)	(sum) (%)
1º	276.3	42.34%	42.34%	36.14%	36.14%	4.03%	4.03%
2º	349.9	0.98%	43.32%	0.21%	36.34%	0.00%	4.03%
3º	351.9	5.16%	48.48%	1.67%	38.01%	0.06%	4.10%
4º	361.2	1.46%	49.94%	0.37%	38.38%	0.01%	4.11%
5º	395.2	31.46%	81.39%	31.91%	70.29%	9.52%	13.63%
6º	513.3	0.17%	81.56%	4.80%	75.08%	0.03%	13.66%
7º	540.6	0.13%	81.69%	0.00%	75.08%	0.00%	13.66%
8º	564.3	0.27%	81.96%	1.14%	76.22%	25.61%	39.27%

9º	616.9	0.43%	82.39%	0.02%	76.24%	0.03%	39.30%
10º	645.0	0.56%	82.95%	0.06%	76.30%	0.03%	39.33%
11º	658.2	0.04%	82.98%	0.02%	76.32%	0.07%	39.40%
12º	660.9	1.06%	84.04%	0.33%	76.65%	0.60%	40.00%
13º	678.2	0.08%	84.12%	0.04%	76.68%	1.88%	41.89%
14º	726.5	0.17%	84.30%	1.91%	78.59%	0.11%	42.00%
15º	748.6	0.37%	84.66%	0.88%	79.47%	0.32%	42.32%
16º	782.1	0.27%	84.93%	2.20%	81.67%	2.18%	44.50%
17º	802.1	0.15%	85.08%	1.70%	83.38%	3.11%	47.60%
18º	811.9	0.06%	85.14%	0.91%	84.28%	1.97%	49.57%
19º	833.5	0.59%	85.73%	0.22%	84.50%	40.36%	89.93%
20º	874.2	0.78%	86.51%	0.99%	85.49%	5.52%	95.45%

Table 7-2 Eigenfrequencies and associated modal effective masses – Rotational DoFs.

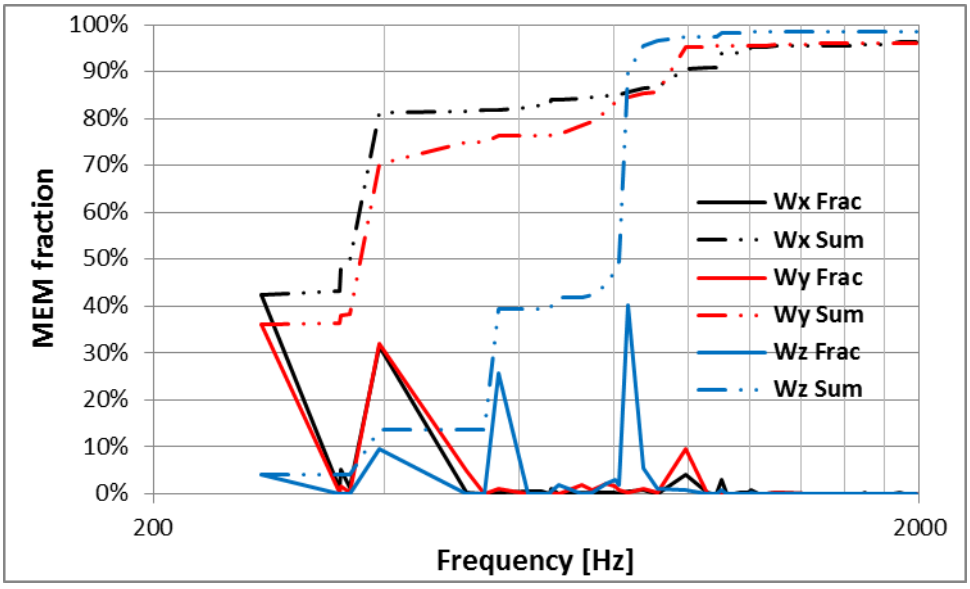

Figure 7-2 Modal effective masses fractional and accumulated – Rotational DoF.

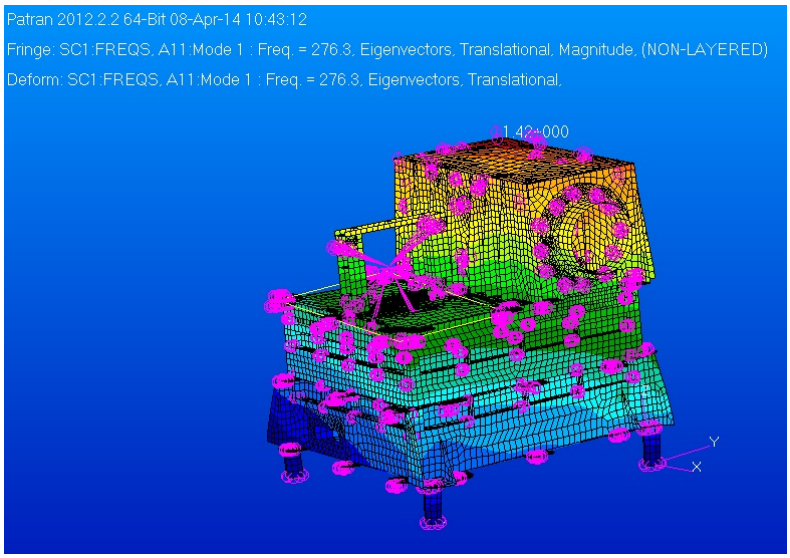

Figure 7-3 First mode (276.3 Hz).

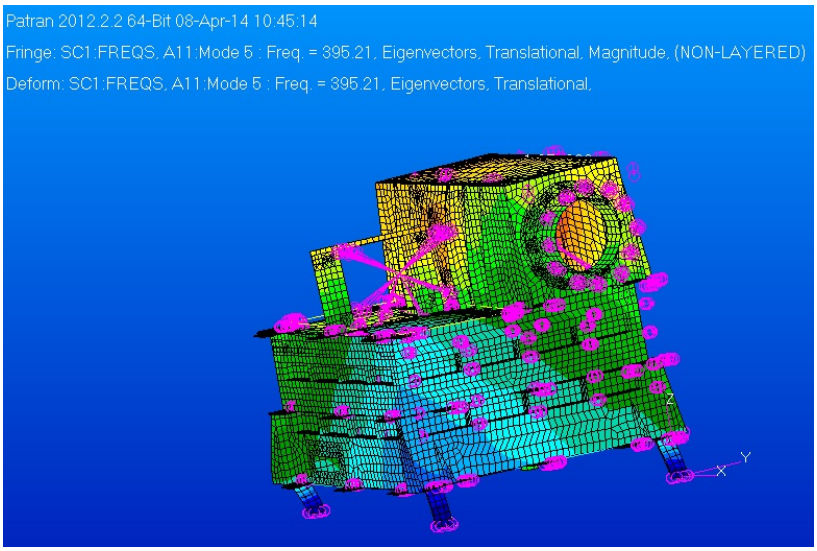

Figure 7-4 Fifth mode (395.21 Hz).

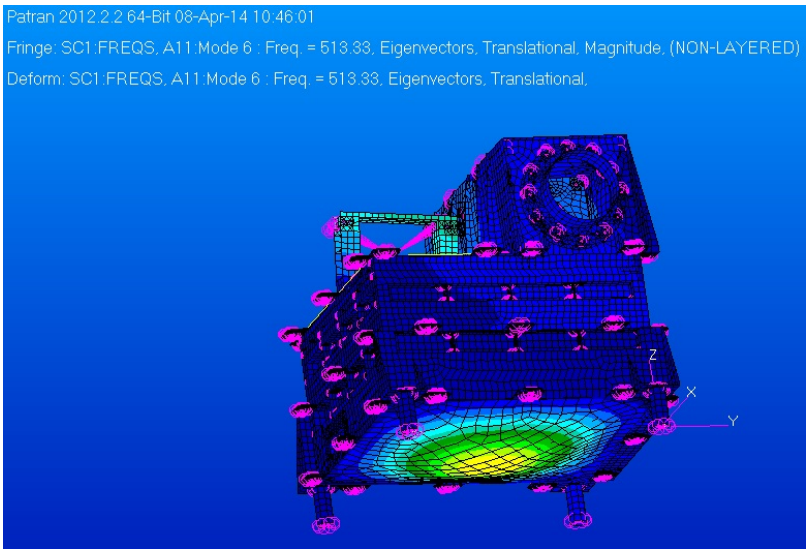

Figure 7-5 Sixth mode (513.3Hz).

7.2 Cuasi-static analysis

Quasi-Static Fail-Safe analysis shall be performed due to the maximum stress levels and I/F forces appear in the combined quasi-static load cases (see section 6.2).

A combined case analysis has been done, combining as out of plane load 69.4g in Z axis and as in plane load $\sqrt{2}\cdot$69.4g in the plane XY. The analyses have been done varying the angle of the in-plane load with the X axis every 45º.

Load Case	Design Load X (g)	Design Load Y (g)	Design Load Z (g)
0º	$\sqrt{2}\cdot$69.4	0	69.4
45º	69.4	69.4	69.4
90º	0	$\sqrt{2}\cdot$69.4	69.4
135º	-69.4	69.4	69.4
180º	$-\sqrt{2}\cdot$69.4	0	69.4
225º	-69.4	-69.4	69.4
270º	0	$-\sqrt{2}\cdot$69.4	69.4
315º	69.4	-69.4	69.4

Table 7-3 Mass acceleration (g).

The SPCs resultant loads can be seen in Table 7-4. They have been obtained recovering the loads with CELAS2 elements (only forces corresponding to translational DoFs have been gathered) and applying safety margins of 20%.

In plane load angle with X axis (deg)	Node: 100000		Node: 100007		Node: 100021	
	In-Plane Load (N)	Axial Load (N)	In-Plane Load (N)	Axial Load (N)	In-Plane Load (N)	Axial Load (N)
0º	610.5	988.5	621.8	724.3	824.3	1564.3
45º	310.4	78.8	646.4	79.1	949.8	1299.9
90º	635.9	829.8	565.4	184.6	750.8	655.0
135º	797.7	1205.0	613.5	87.8	432.7	7.3
180º	582.5	827.1	822.6	736.7	503.9	263.6
225º	409.5	82.6	904.2	1381.9	632.4	0.8
270º	734.0	991.2	771.3	1645.6	528.4	645.8
315º	868.8	1366.4	605.0	1373.2	535.7	1293.4

Table 7-4 Combined Quasi-Static resultant loads X, Y, Z – I/F Forces.

7.3 Bolt failure

The most loaded bolt is bolt 100014 so the boundary conditions on it were eliminated in the analysis. All the calculations are analogous to the section 6.5, with the exception that only yield margins of safety were calculated. The I/F loads are indicated in Table 7-4.

7.3.1 Margin of safety on tensile failure

$$MoS_{tot,y} = \frac{A_s \sigma_y}{F_{V,\max} + \varphi F_A sf_y} - 1$$

In the above expression, the following parameters were used:

- Stress area for the fastener (M5) $\equiv A_S = 1.42 \cdot 10^{-5}\ \mathrm{m}^2$
- Yield stress for Ti 6Al 4V $\equiv\ \sigma_y = 847\ \mathrm{MPa}$
- Maximal guaranteed screw preload $\equiv F_{V,max} = 7400\ \mathrm{N}$
- Force ratio $\equiv \varphi = 0.255$
- Yield safety factor $\equiv sf_y = 1.1$
- Axial load (K_M included) $\equiv F_A$

I/F Point ID.	Load Case	Yield MOS
100007	Quasi-Static 270º	0.52

Table 7-5 Margins of Safety on bolt tensile failure – Minimum value.

7.3.2 No gapping criteria

$$MoS_g = \frac{F_{V,\min}}{(1-n\varphi)F_A sf_g} - 1$$

For this last expression for the margin of safety, the following parameters are defined additionally to those from previous subsection:

- Minimum guaranteed screw preload $\equiv F_{V,min} = 6500$ N
- Gapping safety factor $\equiv sf_g = 1.4$
- Loading plane factor $\equiv n = 0.5$

I/F Point ID.	Load Case	Gapping MOS
100007	Quasi-Static 270º	2.23

Table 7-6 Margins of Safety on gapping – Minimum value.

7.3.3 No sliding criteria

$$MoS_{slip} = \frac{(F_{V,\min} - (1-n\varphi)F_A)N\mu_s}{F_s sf_{ult}} - 1$$

For this last expression for the margin of safety, the following parameters are defined additionally to those from previous subsections:

- Number of bolts of each joint $\equiv N = 1$
- Friction coefficient $\equiv \mu_s = 0.15$
- Total in plane load of the foot (K_M included) $\equiv F_S$
- Axial load (K_M included) $\equiv F_A$
- Ultimate safety factor $\equiv sf_{ult} = 1.4$

I/F Point ID.	Load Case	Sliding MOS
100000	Quasi-Static 0º	-0.01
100021	Quasi-Static 0º	-0.33
100021	Quasi-Static 45º	-0.39
100000	Quasi-Static 90º	-0.03
100021	Quasi-Static 90º	-0.15
100000	Quasi-Static 135º	-0.27
100007	Quasi-Static 180º	-0.24
100007	Quasi-Static 225º	-0.37
100000	Quasi-Static 270º	-0.18
100007	Quasi-Static 270º	-0.30
100000	Quasi-Static 315º	-0.35
100007	Quasi-Static 315º	-0.06

Table 7-7 Margins of Safety on sliding – Minimum values.

7.3.4 Margin of safety on fastener shear failure

In those joints in which the no sliding or gaping criteria is not met, margins of safety for both pure shear and combined shear and axial loads have been calculated. The expressions for the calculation have been the following:

- Pure shear

$$MoS_{S,y} = \frac{\tau_y A_s}{F_S s f_y} - 1$$

- Combined shear and axial loads

$$MoS_{comb,y} = \frac{1}{\left(\frac{F_S s f_y}{\tau_y A_s}\right)^3 + \left(\frac{F_{V,max} + \varphi F_A s f_y}{A_S \sigma_y}\right)^2} - 1$$

For the expressions for the margins of safety additionally to those from previous subsections, the following parameters are defined:

- Yield shear strength $\equiv \tau_y = 491\ MPa$
- In plane load (KM include) $\equiv F_S$

I/F Point ID.	Load Case	Pure shear	Combined shear
		Yield MOS	Yield MOS
100000	Quasi-Static 0º	9.37	1.44
100021	Quasi-Static 0º	6.68	1.34
100021	Quasi-Static 45º	5.67	1.37
100000	Quasi-Static 90º	8.95	1.47
100021	Quasi-Static 90º	7.43	1.50
100000	Quasi-Static 135º	6.94	1.40
100007	Quasi-Static 180º	6.70	1.48
100007	Quasi-Static 225º	6.00	1.36
100000	Quasi-Static 270º	7.63	1.44
100007	Quasi-Static 270º	7.21	1.33
100000	Quasi-Static 315º	6.29	1.37
100007	Quasi-Static 315º	9.46	1.38

Table 7-8 Margins of Safety on fastener shear failure.

8 CONCLUSIONS

A SMM of the EPT-HET instrument has been developed in preparation of the instrument CDR. The model has been validated according to standard procedures. The structural analyses performed show that the instrument structural design is compliant with the applicable requirements.